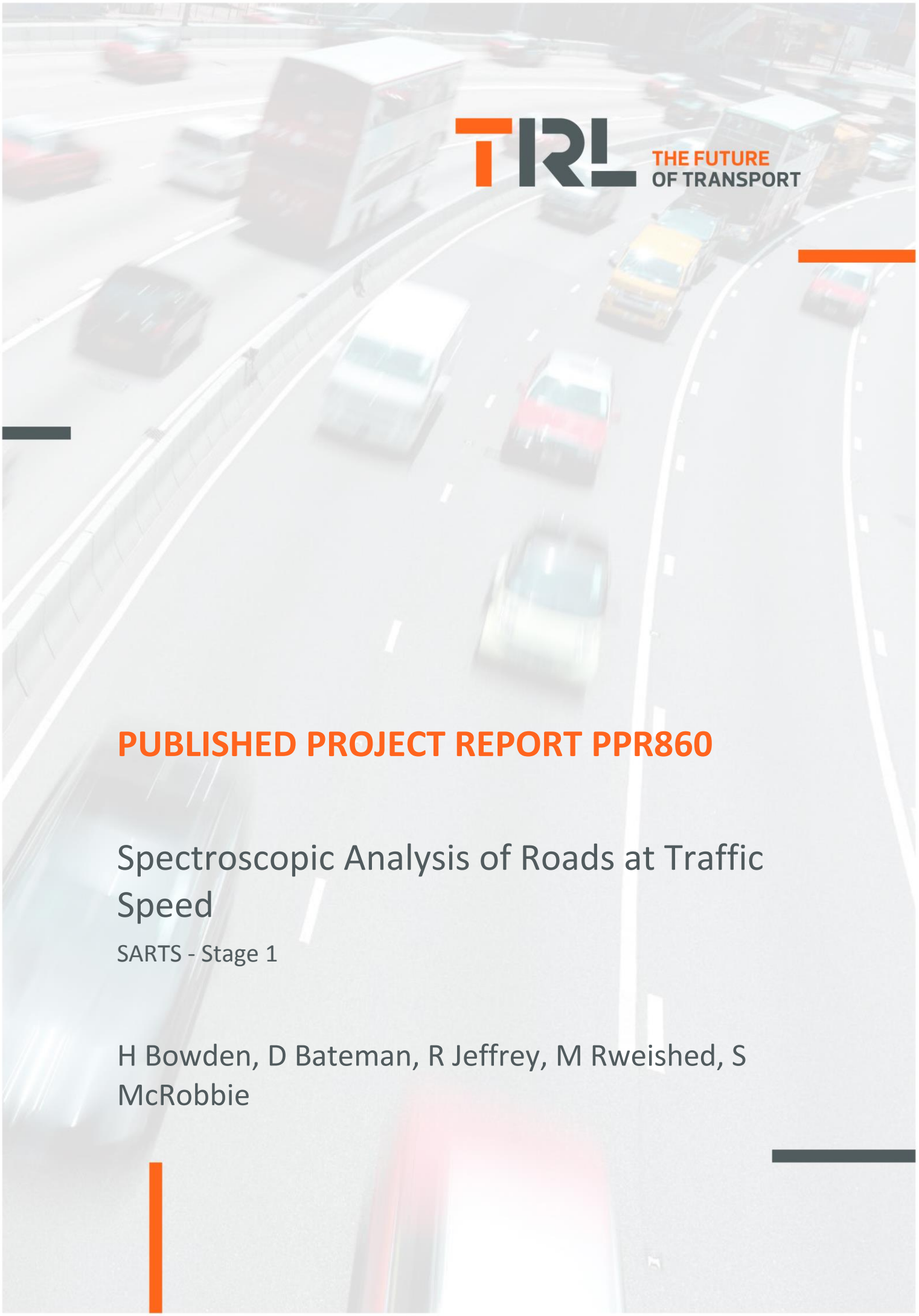

THE FUTURE OF TRANSPORT

PUBLISHED PROJECT REPORT PPR860

Spectroscopic Analysis of Roads at Traffic Speed

SARTS - Stage 1

H Bowden, D Bateman, R Jeffrey, M Rweished, S McRobbie

Report details

Report prepared for:	Highways England		
Project/customer reference:	483(4/45/12)		
Copyright:	© TRL Limited		
Report date:	March 2018		
Report status/version:	1.0		
Quality approval:			
Stuart McRobbie (Project Manager)		Helen Viner (Technical Reviewer)	

Disclaimer

This report has been produced by TRL Limited (TRL) under a contract with Highways England. Any views expressed in this report are not necessarily those of Highways England.

The information contained herein is the property of TRL Limited and does not necessarily reflect the views or policies of the customer for whom this report was prepared. Whilst every effort has been made to ensure that the matter presented in this report is relevant, accurate and up-to-date, TRL Limited cannot accept any liability for any error or omission, or reliance on part or all of the content in another context.

When purchased in hard copy, this publication is printed on paper that is FSC (Forest Stewardship Council) and TCF (Totally Chlorine Free) registered.

Contents amendment record

This report has been amended and issued as follows:

Version	Date	Description	Editor	Technical Reviewer

Document last saved on:	23/05/2018 16:16
Document last saved by:	McRobbie, Stuart G

Table of Contents

1 Introduction

1.1 HE Surveys Background

Highways England and its predecessors have been at the forefront of innovation with regards to traffic speed monitoring of the condition of its pavement asset since the introduction of these techniques in the 1980s. Throughout this period TRL have worked together with HE to provide engineers with data and advice to enable them to make a robust assessment of pavement condition and plan maintenance programmes. As a result of this collaboration, road profile, surface visual condition, structural condition and skid resistance of the Strategic Road Network are now assessed routinely, at traffic speed, as part of the asset management process.

All methods currently used to monitor road pavement condition (visual, TRACS, SCRIM, Deflectograph and TSD) are measuring its mechanical properties and considering its condition at a point in time. The present mechanical condition, very accurately measured, is used to identify those areas of the pavement network where remedial works may be required to restore the life of the road pavement. In the case of Deflection measurements, on some types of pavement construction, they can be used to devise the residual structural life of the existing pavement.

1.2 Project Aims

Previous work for the Highways Agency has concentrated on methods for detecting the early signs of surface disintegration, which is an important deterioration mechanism for modern proprietary surfacing materials, and one that is not detected reliably by current surveys. Proprietary asphalt materials are used extensively on the SRN and significant lengths are at an age where deterioration is to be expected. Deterioration results from weakening of the asphalt over time, through a continuous process of hardening that begins as the asphalt is heated and mixed, continues as it is transported and laid and, at a lower rate, during its lifetime on the road. In the bulk of the asphalt material hardening is beneficial, giving rise to enhanced stiffness, but it is detrimental to the surface course where it can lead to the loss of either bitumen-to-aggregate adhesion, or a loss of cohesive strength in the bitumen, and thereby to surface deterioration. The process is influenced by the nature of the material, exposure to air, water, UV, temperature fluctuations, the presence of various contaminants and traffic.

Many of HE's road pavements are termed 'long life' which means that they have an indeterminate structural life. However they are expected to require regular replacement of the surface course. Road pavement surface courses are a mixture of carefully selected and specified aggregates held together with bituminous binder and a small amount of additives such as polymers and fibres. The surface of the road fails through the attrition and/or weathering of the materials of which they are made. As the chemical composition of the binder changes through the effects of ultra violet light, oxidation and weathering it becomes more brittle and also loses adhesion to the aggregate. As a result the pavement surface

breakdown under the action of traffic when the binder loses either internal cohesive strength or adhesion to the aggregate.

1.3 Previous work done in the industry

This project will develop the methods for measurement of the change of the chemical composition of the pavement surface, particularly the binder, and relate those changes to the expected remaining service life of the pavement. An Arup-URS feasibility study has indicated that the understanding of the chemistry of bituminous binders and the technology for performing a remote spectrographic analysis of the road surface now exist (Widyatmoko, 2014). It also identifies the areas of research that are required to apply the technology and to develop the prediction model for the remaining life of the road surface. The final task in the feasibility study is to carry out road trials of the new methodology and technology to warning indicators that can be used by engineers and administrators to monitor the remaining life of the road pavement surface and plan remedial works and funding requirements.

Asphalt fretting occurs due to chemical and physical changes in the asphalt surfacing which can be caused by a combination of poor construction quality, environmental effects, and trafficking (Francken, 2004). Environmental factors include temperature changes, moisture damage, and exposure to Ultra-Violet (UV) light, all of which change the chemical and physical behaviour of asphalt mixtures. This behaviour is often referred to as age-hardening or ageing of asphalt and has been well documented in previous research (Read, 2003). Increased oxygen levels lead to an increase in viscosity and a decrease in cohesion between the aggregates and the bitumen, resulting in reduced elasticity and greater stiffness. Whereas ageing of underlying asphalt (structural) layers can greatly improve the overall strength of the pavement structure, ageing of the surface layer reduces the cohesive and adhesive properties of the mixture. Aged surfacings are then at risk of mechanical damage from trafficking whereby aggregates are easily displaced from the surfacing (Francken, 2004). High levels of oxidation that occur during the mixing (plant), transportation, and laying of the asphalt mixtures are often referred to as short-term ageing while oxidation that occurs during the pavements' service life is referred to as long-term ageing.

1.4 Project overview and objectives

This paper presents an alternative approach to evaluate changes in asphalt mixtures through the use of infra-red spectroscopic testing and analysis, combined with established and newly developed laboratory test methods. The following research areas will be explored:

Spectral Analysis of Bitumen, Aggregates and Contaminants

- Assessing the application of IR spectroscopy for road surface monitoring
- Identify and fingerprint common road surface contaminants
- Identify and fingerprint common bitumen grades and sources with age.
- Identify and fingerprint common aggregates used in pavement surfaces
- Investigate spectral changes with ageing of bitumen and asphalt.

Infra-red Spectrographic analysis Technology

- Initial assessment of technology capability and potential to perform in motion.
- Develop DR-FTIR technology for use in motion
- Laboratory/field testing and analysis of off road sites, and cores including HRA and TSC materials.
- Develop method of sample collection and frequency of measurements required

Mechanical testing of aged samples

- Age Samples using laboratory techniques, UV and naturally.
- Develop a bespoke shear test for asphalt samples
- Carry out penetration and softening test on bitumen samples
- Carry out Vialit pendulum tests on asphalt and bitumen samples

2 Methods used for aging samples

2.1 Laboratory Ageing

There are different types of laboratory tests that simulate the performance of in-service asphalt mixtures which include accelerated aging of the bitumen, the loose asphalt mixture, or of the compacted asphalt samples. For bituminous binders, there are three European standardized tests for short-term ageing at high temperatures, namely Rolling Thin-Film Oven Test (British Standards Institution, 2007), Thin Film Oven Test (British Standards Institution, 2014), and Rotating Flask Test (British Standards Institution, 2007). These tests reasonably simulate asphalt ageing particularly during the mixing and transportation stages.

With regards to long-term ageing, laboratory simulation is much more difficult. Ideally, laboratory testing should be able to replicate changes to the chemical and physical properties in the bitumen in an asphalt pavement after some years of service. Some studies suggest that this can be achieved by using artificially severe conditions i.e. temperatures much higher than in-service temperatures and pressures much greater than ambient pressure. The two most common methods for simulating long-term ageing tests are Pressure Aging Vessel (British Standards Institution, 2012) and the Rotating Cylinder Ageing Test (British Standards Institution , 2007). However, there is very little evidence to support the relevancy of these methods considering their severity and how it relates to natural ageing of in-service asphalt. Indeed, it has been suggested that ageing of bitumen at a higher temperatures may be fundamentally different from ageing at lower temperatures which are typically associated with the ageing of in-service pavements (Branthaver, 1993).

As a result of the limitations associated with laboratory test methods in estimating the long-term performance of asphalt surfacing, it becomes more important to monitor the performance of in-service roads. A novel approach to this problem employs infra-red spectroscopy.

2.2 UV box Ageing

A UV chamber, which contained 8 Sylvania UV lamps, was developed for the artificial ageing experiments (Figure 1). The temperature within the chamber was maintained at 60˚C for the duration.

Figure 1: UV Ageing Chamber

A sample of 40/60 penetration-grade bitumen was used for these ageing experiments. The bitumen was poured into four penetration pot tins and placed into the UV chamber. One sample was removed at weekly time intervals and reflectance spectra were taken from the surface. This procedure was repeated for three weeks. One sample of bitumen was placed into the chamber and was covered so that it was not exposed to the UV light. This sample was removed after three weeks and spectra were obtained from its surface. Three further bitumen samples were prepared in the same way and were placed onto the roof of the Transport Research Laboratory headquarters at Crowthorne House, Berkshire, UK. These samples were exposed to natural conditions of UV exposure, rainfall and temperature fluctuations; these parameters were monitored by a weather station.

A systematic approach was employed to monitor the oxidation of raw bitumen samples as they were naturally aged and aged artificially using the UV chamber. This allowed for the oxidation product absorbance bands to be identified. Following this, asphalt samples were produced that were representative of in-service road surfacing mixtures.

2.3 Natural Ageing

A Stone Mastic Asphalt (SMA) mixture, supplied by United Asphalt, was used in this study. This mixture type contained 100/150 penetration grade binder. From this mixture, asphalt slabs were compacted and produced in compliance with (British Standards Institution , 2016). These slabs contained a maximum aggregate size of 10mm and a binder content of 6%.

A number of these asphalt slabs were placed on the roof of Crowthorne House in August 2015 and have been exposed to 24 months of natural ageing at the time of this publication. An asphalt slab was removed from the roof at specific time intervals, approximately 3 months apart. The DRIFT spectra were collected from the surface of the asphalt samples and mechanical testing was carried out on the recovered bitumen.

3 Measurement of mechanical properties of pavement materials

3.1 Mechanical property testing of raw bitumen

The mechanical properties of the raw bitumen samples were measured using the penetration test (British Standards Institution , 2015), the Softening point (British Standards Institution , 2015) and the Vialit pendulum test (British Standards Institution, 2008). All mechanical property testing was performed at the Surrey County Council, Highways and Transport, Materials Laboratory.

3.1.1 Penetration and Softening test

The specification for the penetration point test can be found in the British Standard (British Standards Institution , 2015). It is described as a method for measuring the distance, in tenths of a millimetre that a standardised needle with a 100g loading weight penetrates vertically through a sample of bitumen held at 25˚C in 5 seconds. This is the experimental set up for penetration values up to 300 x 0.1mm however the temperature drops to 15˚C for penetrations above this value. Experimentally the distance that the needle travels through the bitumen decreases as the bitumen ages. This very simple and easy test will be used in this project to measure a change in the mechanical properties of the aged bitumen. By taking an IR spectrum of the bitumen at each time point and observing any changes could lead to a link between the mechanical deterioration of the bitumen and a change in the chemical composition. Figure 2 shows a very simplistic diagram of this experiment.

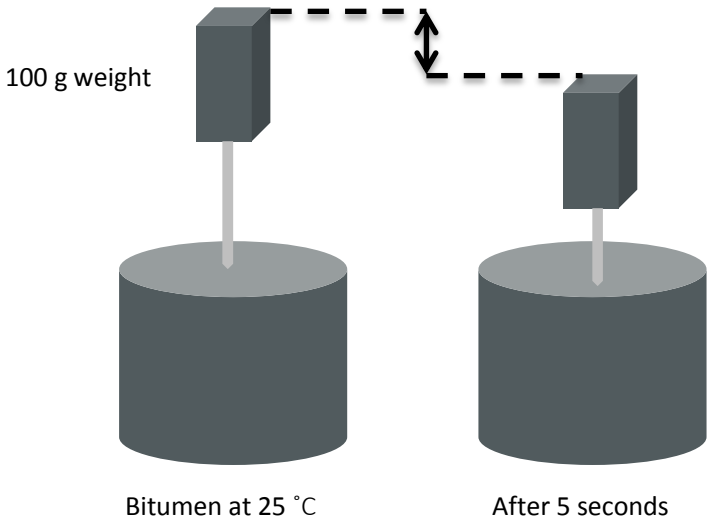

Figure 2: Diagram representation of penetration point testing

The softening point of the bitumen is the temperature at which the sample reaches a specific consistency and is measured using the Ring and Ball method detailed in the British Standard EN 1427. This is done by heating two discs of bitumen at a constant rate in a liquid bath of either water or glycerol. These two discs are each supporting a standardised steel ball and the softening point is the average temperature at which the bitumen discs allow the

ball to fall a distance of 25±0.4mm. As the binder ages the softening point temperature increases as the binder becomes less viscous at lower temperatures. See Figure 3 for a simplistic representation of this experiment.

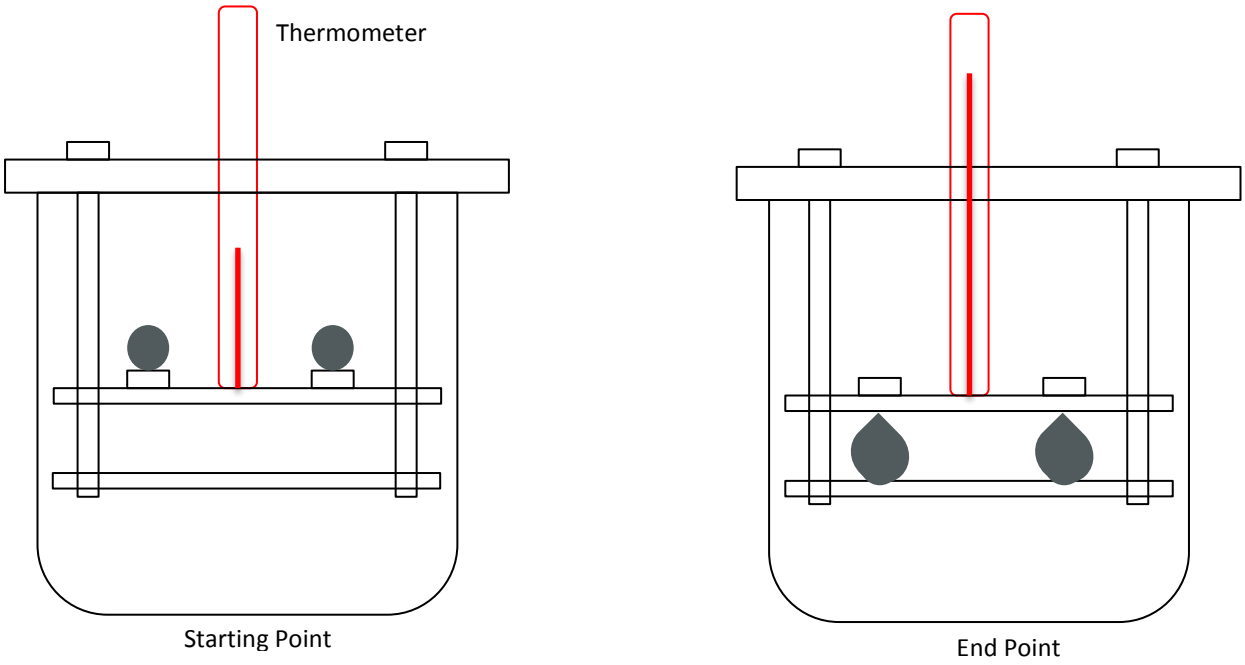

Figure 3: Diagram representation of softening point testing

3.1.2 The Vialit Pendulum Test

Another mechanical property of the bitumen that is of interest in order to predict the quality of road structure is the cohesion. Cohesion is very important between the binder and the aggregates and also within the binder. A decrease in the cohesion may lead to the road surface suffering rutting and fretting failure mechanisms. The pendulum test is designed to measure the energy per unit area required to detach a standardised steel cube that has been adhered to a support with a thin layer of bitumen. A number of repeats across a range of temperatures are carried out in order to find the temperature at which the cohesion is the highest. In this experiment a 1cm^3 steel cube is attached to a 1mm thick sample of binder and bound to a steel support. This is then brought to the test temperature and a pendulum is released. This then hits the small cube and detaches from the bitumen. The angle that the pendulum reaches after contact is recorded and the cohesion is calculated. The test is standardised with full specification being published in the British Standard EN 13588:2008. A diagram of the test set up can be seen in Figure 4.

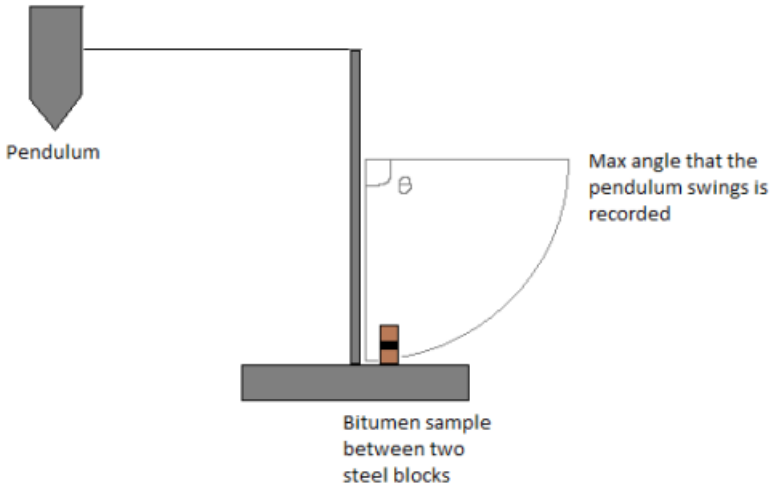

Figure 4: Vialit pendulum test set up

There are a number of variables in the experiment that could lead to results which are difficult to reproduce. The sample that is being analysed has to be brought to temperature then hit with the pendulum within 20 seconds. The decreasing temperature upon removal from heat source could lead to variation within results. The pressure used to adhere the steel block to the binder must remain constant between samples otherwise this could produce unreliable results.

3.2 Mechanical property testing of asphalt mixtures

As stated earlier, there are limited test methods which evaluate the cohesive and adhesive properties of bulk samples, particularly for surface course mixtures. Flexural testing has been used in the past as a means to understand the effects of ageing on asphalt materials. However, flexural testing assesses the stiffness of compacted asphalt mixtures rather than the cohesive properties between the binder and the aggregates in the surfacing. Therefore, there is a need to develop a test method that characterises the loss of aggregates from reduced cohesion within a bulk sample due to UV ageing.

The asphalt shear test is based on the shear strength test for soils (British Standards Institution , 1990), which is used as a tool to measure soil cohesion, and is modified for asphalt mixtures. Figure 5 presents a schematic of the asphalt shear test device and illustrates how it is used with the Instron universal testing device. The sample is positioned in the clamp such that the lower clamp is 15mm from the edge of the sample and the upper clamp is 10mm back from the edge of the sample. This positioning exposes the maximum size of aggregate (10mm) to loading, and allows the sample to crack at its weakest point i.e. voids and failure of the aggregate-binder bonds rather than cracking through aggregates. Once the shear test device is fixed in place the blade is lowered at a constant rate and the sample is subjected to load until it fails.

Asphalt samples of dimensions 150mm x 10mm x 40mm (LxWxH) were cut from the compacted slabs. Initial testing was performed on four different asphalt slabs, all containing the same asphalt material (10mm maximum size aggregate) with 10 samples cut from each slab. The bituminous core density, maximum density, and percentage air voids was

determined for each sample, in accordance with BS EN 12697 Parts 5, 6 and 8 (British Standards Institution , 2009) (British Standards Institution , 2012) (British Standards Institution, 2003), prior to shear testing. Samples from each slab were divided up with half of them exposed to UV light for one week while the other half were also placed in the UV chamber but not exposed to UV light. This was done to assess the effects of UV ageing only with all samples exposed to the same temperature (60°C). The samples and equipment were then conditioned at 20°C (overnight) and then tested at ambient room temperature (20±1°C).

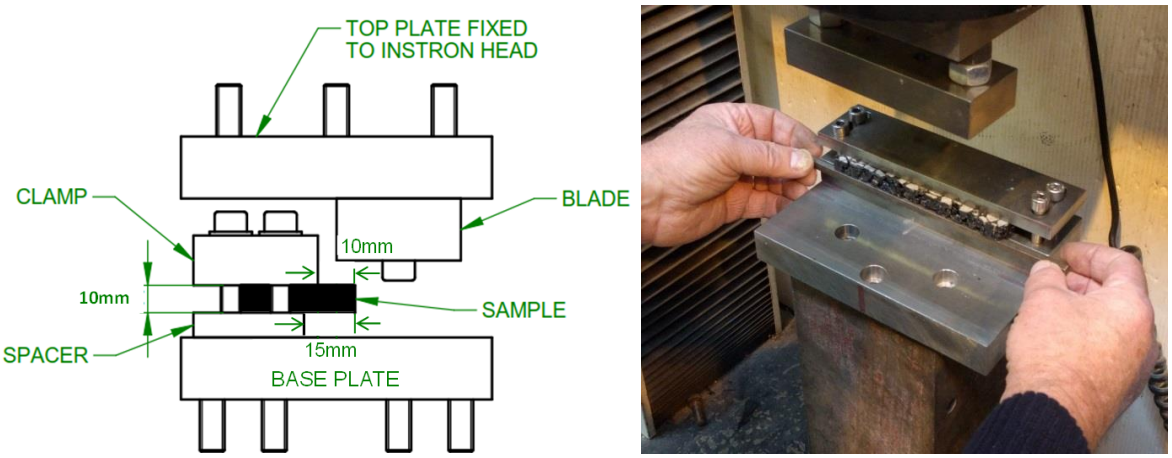

Figure 5: Asphalt shear test set-up

4 Spectroscopic measurement of pavement materials

4.1 Infra-Red spectroscopic analysis

4.1.1 Infra-red Spectroscopy background

Infra-red (IR) spectroscopy works by irradiating an asphalt sample with a beam of infrared radiation and measuring how much of the light is absorbed. It is possible to determine which heteronuclear bonds are present within the sample as each bond will absorb a specific wavelength of light to initiate a vibration of the bond. The absorbance bands present in the infra-red spectrum of a sample can then be used to identify the bonds present in the sample.

Several studies have related changes in the infra-red spectroscopic signals to changes in physical properties of bitumen (Lu, 2002) (Saoula, 2013). These reports monitor the presence of oxidation product absorbance bands in the Attenuated Total Reflectance-Fourier transform Infra-Red (ATR-FTIR) spectra collected from aged bitumen. ATR-FTIR spectroscopy requires good contact between the sample and a crystal that has a refractive index higher than the sample being analysed.

Although there are many fundamental spectroscopic studies on bitumen, there have been minimal studies carried out on the oxidation of bitumen when it is a component of asphalt. As asphalt is a mixture of bitumen, calcium carbonate filler and aggregates, the spectra are predicted to be a complex mixture of absorbance bands from all of these components. This makes the absorbance band assignment of the infra-red spectra more difficult.

The hard, rough surface of the asphalt also means that a non-contact measurement must be employed; diffuse reflectance infrared spectroscopy in this case.

4.1.2 Fourier Transform Infra-Red Spectroscopy & Diffuse reflectance spectra of asphalt samples

Fourier Transform Infra-red (FTIR) spectroscopy is a very well established analytical technique that is able to analyse solids, liquids and gasses as a non-destructive technique. For these reasons it extends itself to many different fields. A few examples include forensic identification of trace evidence from explosives to paint, pharmaceutical quality control of drugs, and even archaeological examination of building materials from sites around the world. FTIR can be a portable technique which means it can produce very rapid and simple sample analysis in the field, away from the laboratory.

The most common spectrometer design is the Michelson Interferometer that works by shining a beam of infra-red light towards a beam splitter which splits the beam of light in two directions. One portion of this light is directed towards a stationary mirror and the other portion towards a mirror that is moving at a specific rate through a set path length. The light is then reflected back to the beam splitter where it recombines and experiences an amount of interference depending upon how out of phase the beams are due to the increased distance one beam had to travel. The light is split again and part of this travels to a sample container and the other is transmitted back to the source. As the beam passes

through the sample some wavelengths of light are absorbed and some are transmitted through to the detector. This is followed by some complex Fourier Transform mathematics and the interferogram produced by the spectrometer is converted into a spectrum that displays intensity vs. frequency.

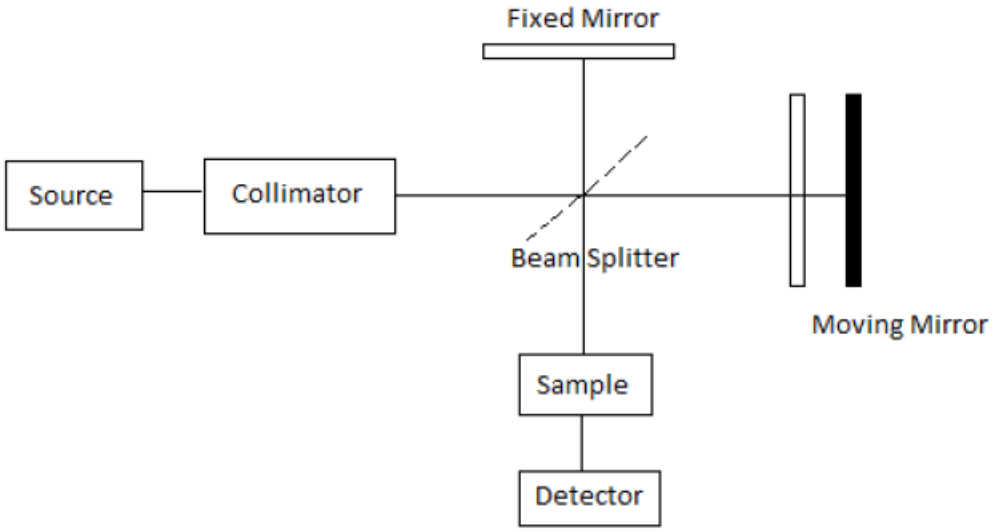

Figure 6: Michelson Interferometer Infra-red operation schematic

As opposed to ATR which requires a good contact between the sample and an ATR crystal, diffuse reflectance involves collecting light that has been scattered by a sample. The light can be scattered in many directions depending upon the microstructure of the surface. If the sample is very shiny then the light is scattered at an angle that is equal to the incident angle however if the sample is dull then the light is scattered at angles that are different to the incident angle. This light can be collected by a diffuse reflectance detector and processed through the Michelson interferometer to produce a Diffuse Reflectance Infra-Red Fourier Transform (DRIFT) spectrum.

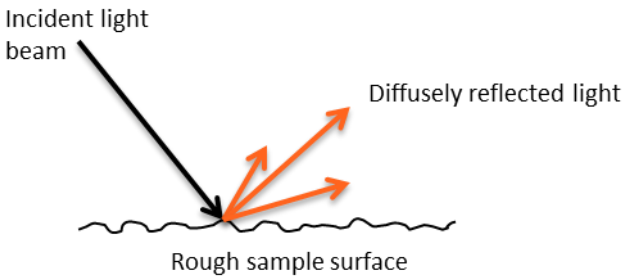

Figure 7: Diffuse scattering of light from a rough surface

Reflectance spectra have a characteristic appearance which can be complex. Many bands in DRIFT spectra have a low signal-to-noise ratio as a result of an increased path length for the light beam reducing the intensity of the absorbance bands.

If the sample is shiny, this leads to an increase in the amount of specular reflectance that leads to distortion of absorbance bands in the reflectance spectra. The observed spectrum will therefore be a sum of the diffuse and specular reflectance character of the detected light. First derivative peaks are often observed in specular reflectance spectra when there is

a change in absorbance due to a change in refractive index as the IR beam moves through a range of wavelengths (Spragg, 2013). In interpreting these spectra it should be noted that the vertical axis shows reflectivity and lower values of reflectivity indicate a higher absorbance.

The infrared spectroscopic analysis on all samples was carried out using an ExoScan 4100 hand-held spectrometer (Figure 8).

Figure 8: Agilent Exoscan 4100

The Exoscan 4100 can be utilised to measure Diffuse Reflectance FTIR with a specialised detector head attachment. The diffuse reflectance attachment allows a small distance the detector and the sample. This means it can analyse a rough surface as no contact is required between the detector and the sample. The reflectance spectra reported are an average of 64 scans with an 8cm^{-1} resolution

4.2 Instrumental noise

The spectrum shown in Figure 9 is formed of 128 individual scans using the Exoscan spectrometer. One scan is a single pass through the frequency range of the instrument, and can produce a single spectrum. The Exoscan Spectrometer control software allows the user to select a number of scans to be averaged together to produce the final spectrum. Though this gives an improved signal to noise ratio, it comes at the cost of significantly increased integration time; to collect a spectrum featuring over 100 scans may take 60 seconds or more.

In consequence, there are two reasons that the variation between individual scans at the same site is of interest. Firstly, understanding this variation allows a measure of the instrumental variability. Secondly a trade-off must be made between speed of data collection and the required signal-to-noise ratio. This is particularly true in a system operating at traffic speed, where a vehicle travelling at 50 miles per hour covers 22 metres of pavement each second.

Figure 9 shows a spectrum consisting of only a single scan. The spectrum is noisy, with few of the features seen in Figure 10 visible. Note also the several spikes where the absorbance is reported as 5; recall that absorbance is a logarithmic scale, where high values mean less

light returns to the detector. These spikes correspond to instances where insufficient light is returned for a value to be recorded.

Looking at Figure 10, 128 single-scan spectra are plotted on the same axes, together with their mean spectrum. The grey band indicates the combined spread of these scans – the significant variation from sample to sample is clear. However, it is also clear that the single averaged spectrum provides a good representation of the spectrum across a wide range of light frequencies.

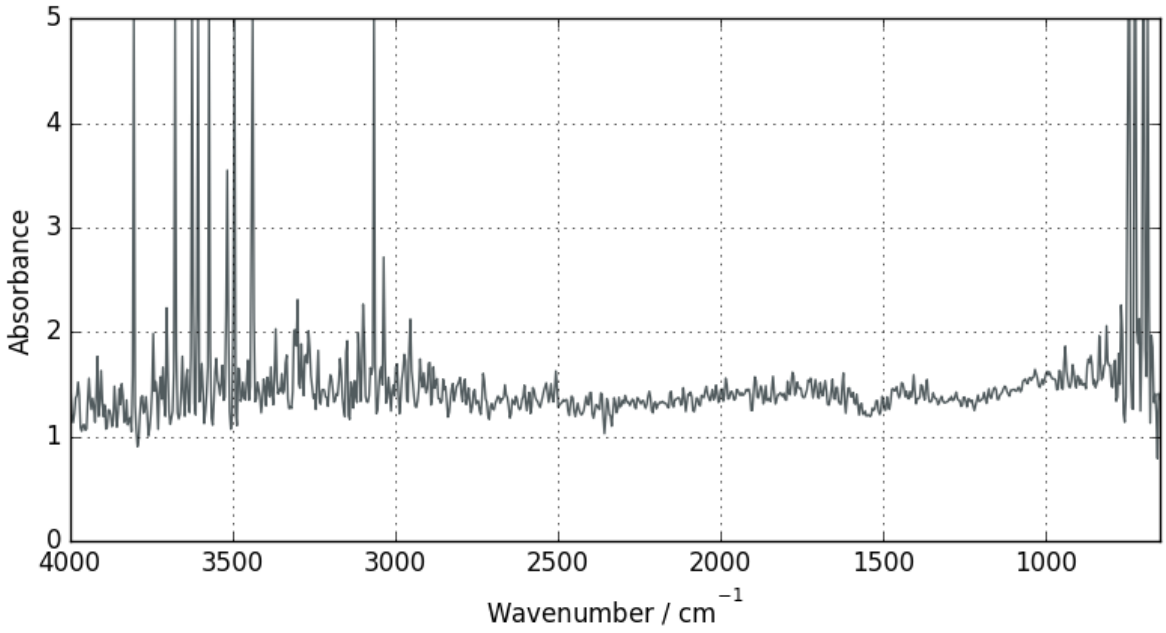

Figure 9: Single-Scan FTIR spectrum taken from a pavement core sample with Exoscan Spectrometer

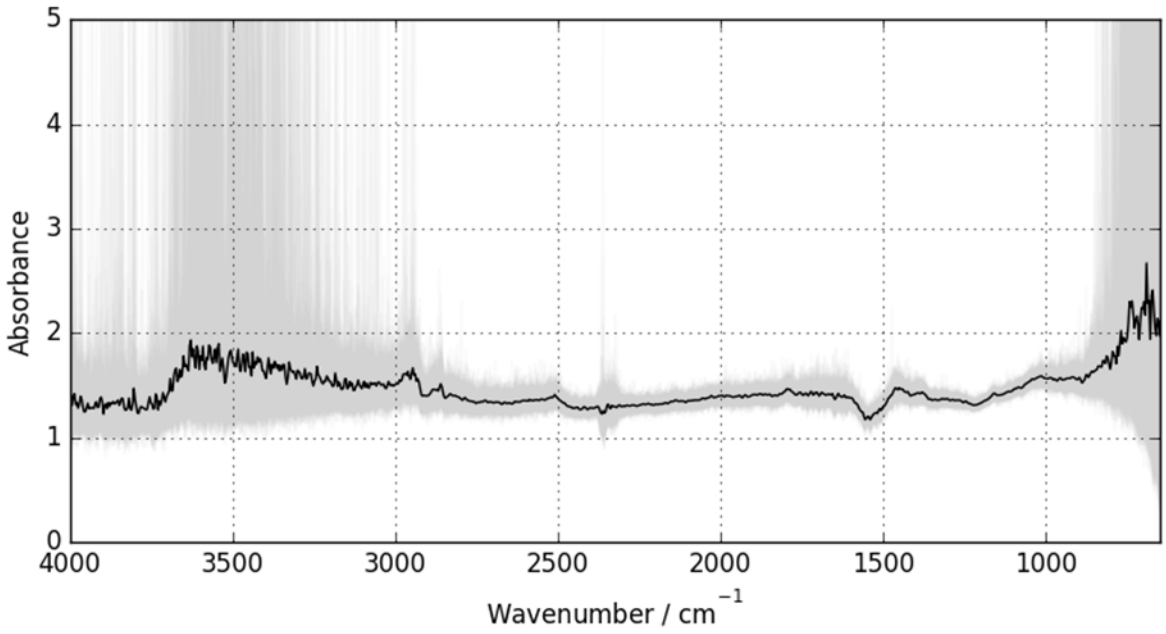

Figure 10: 128 single-scan spectra taken at the same location on a pavement core, together with the sample mean. The width of the grey band indicates the range of absorbance values at each wavelength

4.3 Background subtraction & temporal drift

The Exoscan Spectrometer uses a background subtraction to set the baseline level of the spectrometer. This accounts for the spectrometer response, as well as helping to remove environmental effects.

To do this, a spectrum is taken of a diffuse reference sample with a flat spectrum across the mid-infrared range (4000cm^{-1} to 650cm^{-1}). A number of different reference caps are provided with the spectrometer. Two of these caps (the 100 micron diffuse cap and a rough gold cap) can be used to set this background. Though both provide a reasonably flat and featureless spectrum across the mid-IR range, their overall reflectance differ (the gold cap is more reflective than the 100 micron sample), meaning that spectra taken with the two reference methods cannot be quantitatively compared.

A third, polystyrene reference cap is provided for calibration of the internal reference laser frequency. Unlike the other two, this has a feature-rich spectrum with known spectral lines that can be used to reference the laser frequency. This won't be discussed further here.

There is a parameter defined within the method that allows the user to select how often a background measurement should be taken. This may be set to require a background measurement before each individual science spectrum. However, each background measurement is a time-consuming exercise, requiring the user to remove the spectrometer from the sample, attach the reference cap, wait for the spectrum to finish collecting (which may take a minute or more), and then return the spectrometer to the sample. This is inconvenient, and would become impossible in a real-world implementation. The importance of background measurement will be assessed next.

The rough order-of-magnitude of this effect can be gauged semi-quantitatively by the following simple experiment, which monitors changes in the background over a period of several hours. The spectrometer is set up in the lab and a background spectrum is taken. For the purpose of this experiment, the 100 micron reference was used, and the number of scans (both per spectrum and for the background measurement) was set to 256 (this could be done because, while measurement time was not an important consideration, minimising noise to obtain a clean spectrum would allow comparison across times). Then, without the background calibration, the spectrum of the 100 micron reference cap was re-measured.

If the background remained stable, the spectra would be expected to remain flat. However, if there is instrumental drift, or a change in the environment, this should manifest itself as a deviation from zero absorbance.

Five of the resulting spectra are shown in Figure 11. The background was collected at 0932hrs, and the first spectrum (top panel) taken immediately thereafter; as expected, this spectrum is flat. Spectra were taken repeatedly over the following hour, and then sporadically until 1600hrs. It is clear that there is a significant change in the absorbance values, with absorbance values as high as 0.15 (i.e., 30% absorption) seen at some wavebands. The origin of these features is easily understood – the two broad features at 4000cm^{-1} – 3500cm^{-1} and at 2000cm^{-1} – 1300cm^{-1} are water absorption peaks, while the feature at 2350cm^{-1} is carbon dioxide. Note that the sharp peaks seen within these bands are physical, not random: these are vibrational features of the water molecule.

The general continuum level also varies during these observations, drifting away from 0 to absorbances of perhaps as great as 0.025 (5% absorption).

A different representation of this time evolution is given in Figure 12, where the absorbances at 17 different wavenumbers are plotted as a function of time. These are chosen to correspond to peaks in the water spectrum, and to represent the continuum level. In the first part of the experiment, these all display a smooth evolution, before plateauing out by about 3 hours after the start of the experiment.

This behaviour is well explained as due to carbon dioxide gas and water vapour exhaled by other workers within the lab during the course of the working day, increasing the levels of these gases from those at 0930hrs when the initial spectrum was taken. By about 1230hrs (i.e., 3 hours after the experiment began), these appear to have reached equilibrium/saturation levels.

This simple experiment does not lend itself to a more precise analysis than this. This is because it features (at least) two parameters that change with time – namely instrumental drift and environmental drift -- and which have not been controlled for or tested independently. Accordingly, their effects can't be disentangled. However, in spite of the limitations of the test, it still suggests the following plausible hypotheses.

1. It is most likely that environmental effects due to varying densities of water vapour dominate this experiment. It is concerning that the variation seen in this exercise (up to 0.12) is comparable to the changes seen in bitumen samples, especially given that the water feature between 2000cm^{-1} and 1200cm^{-1} is in the region containing a number of spectral features of bitumen.

In a real world implementation, there are likely to be variations due to changes in humidity, and, given that water vapour is a waste product of the combustion engine, there may be variations due to changes in traffic conditions. Further testing may be needed to gauge the magnitude of this effect.

Note also that the change seen here occurs only due to variations along the very short optical path between detector and a reference cap fixed to the opening of the spectrometer. In a traffic speed implementation, with the detector at a distance from the pavement, the optical path will be greater. From Beer's Law, the absorbance scales linearly with both density of absorbers and optical path length. This may increase the effect by an order of magnitude.

These observations of environmental effects point to two things: firstly, that the system will need to be calibrated often (to remove the effect of environmental drift; and secondly, that in a stand-off system, atmospheric water vapour along the line-of-sight will be a significant constraint on the system's operational capabilities between 2000cm^{-1} and 1200cm^{-1}.

2. The effect of instrumental drift is still unclear, as environmental changes dwarfed any instrumental time dependence in this experiment. To measure this properly, the experiment would have to be repeated in a climate-controlled environment. Ultimately though, this is not important, if the final system uses different optics to the Exoscan. However, qualitatively, it seems likely that the effect is small, as shown by the development of an equilibrium state.

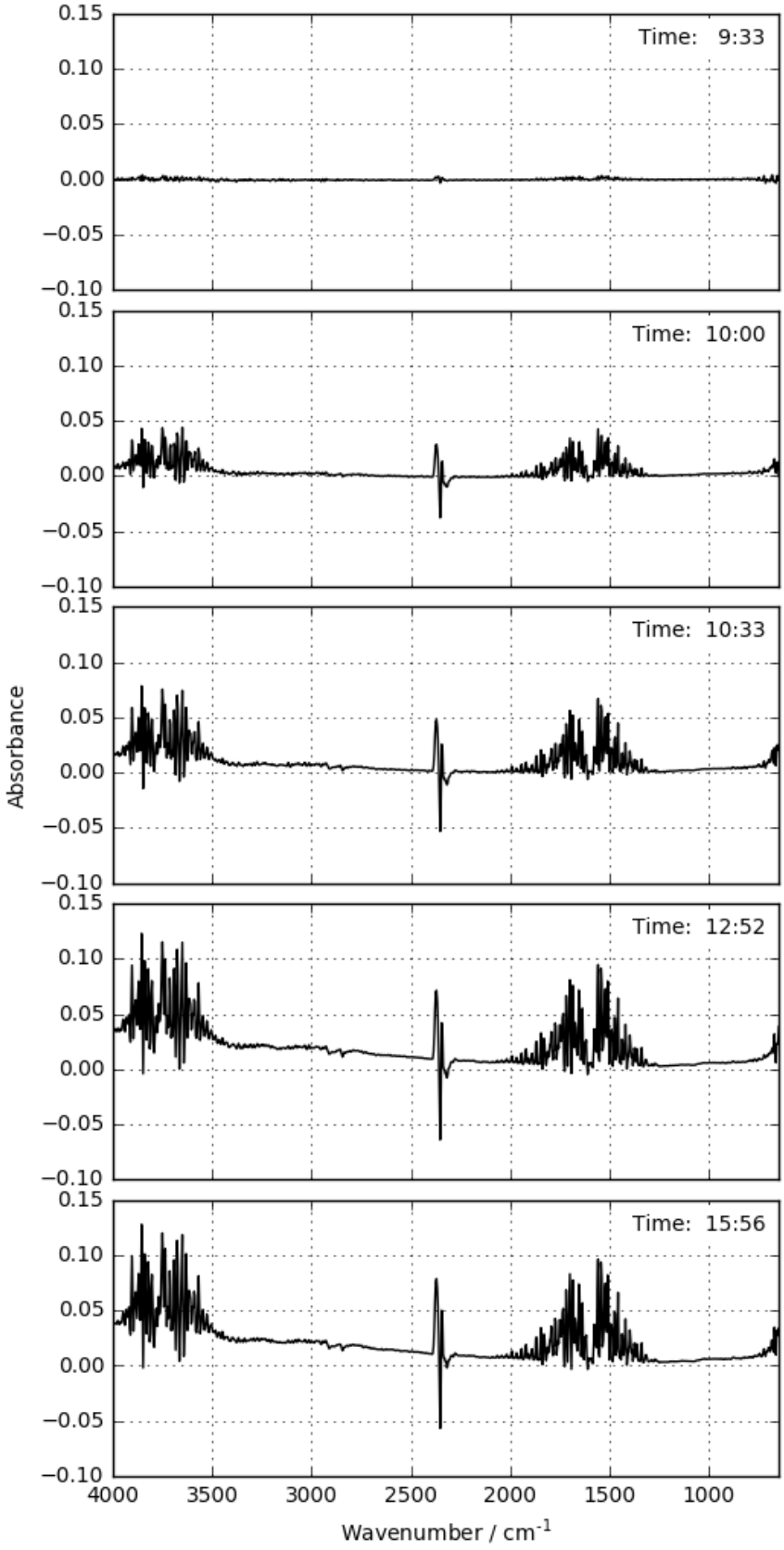

Figure 11: Drift in the background spectrum of the Exoscan Spectrometer over 6.5 hours.

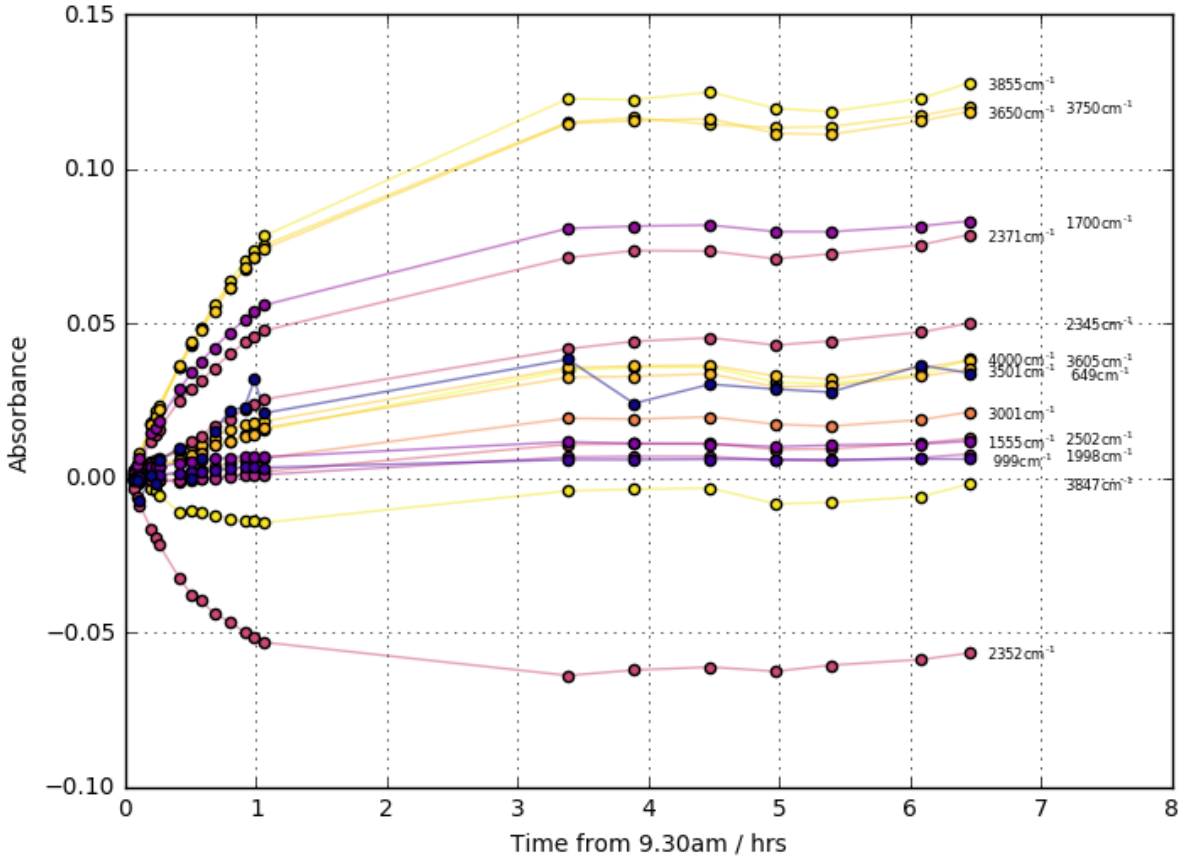

Figure 12: The time evolution of the background absorbance at different wavenumbers. The colour of each line is scaled by its position within the mid-IR waveband. An initial rise is seen, which reaches an equilibrium value by about 3 hours after the experiment begins

4.4 Field-of-view

An understanding of the size and shape of the field-of-view of the Exoscan spectrometer is needed to allow the user to interpret the resulting spectra by matching spectral features to structures in the sample.

The field-of-view can be estimated in a simple experiment in which two substances with contrasting spectra are used to define an edge. In this experiment, this was achieved using a 30mm wide strip of paper set against a foam background. The spectrometer is then moved over the edge, using a moving table test rig (Figure 13).

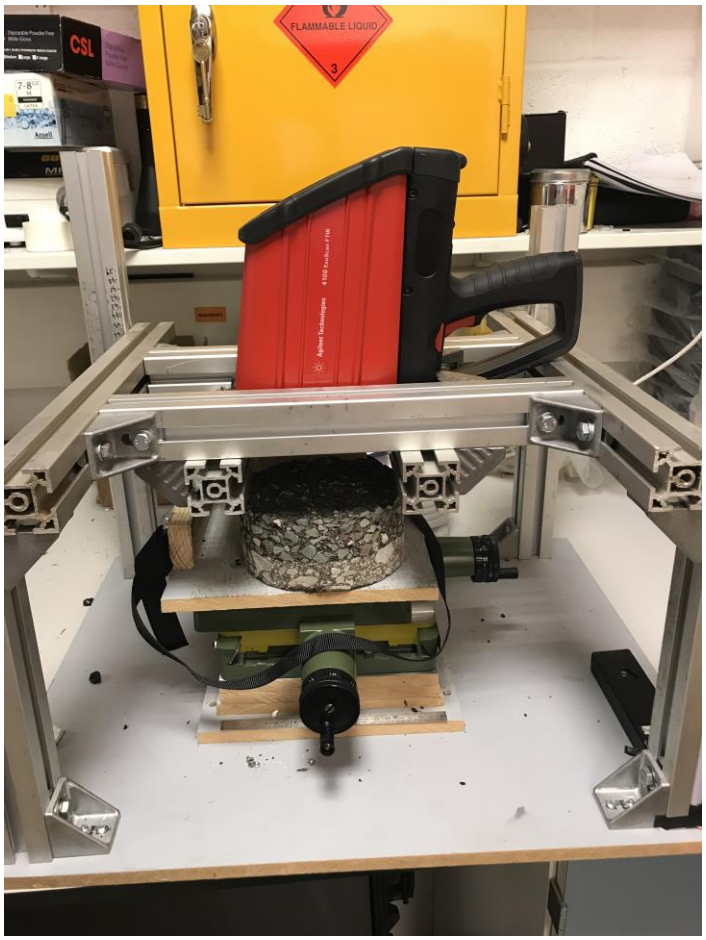

Figure 13: Exoscan precision table test rig

Spectra are taken at appropriate intervals, and the positions recorded – this was varied between 4mm (away from the edge) and 0.25mm (over the edge). A representative wavenumber was picked (2080cm^{-1}), and the absorbance at that wavenumber plotted as a function of position. This is shown in Figure 14. The transverse profile was collected by moving the sample left-right past the spectrometer, then the sample was rotated through 90 degrees to allow the longitudinal profile to be measured by moving up-down. The two profiles were aligned on the midpoint of the trough. The expected shape of this profile is a "top-hat" function convolved with the approximately Gaussian shape of the field-of-view (the "beam"), giving two step functions with smoothed sides. This is as seen. An estimate of the beam size is taken from the width of the sides of this step. In both longitudinal and transverse directions, this is approximately 1mm.

Though of slightly academic importance to any real world application -- which is unlikely to use the same optical arrangement as the Exoscan – this estimate will be used in the next Section where the spectrometer is used as a crude spectral imaging camera.

Note that this hasn't determined the depth of focus – qualitatively, it is observed that this device has a restricted depth at which it can collect quality spectra (perhaps less than a few mm). The final design will need more flexibility in this regard.

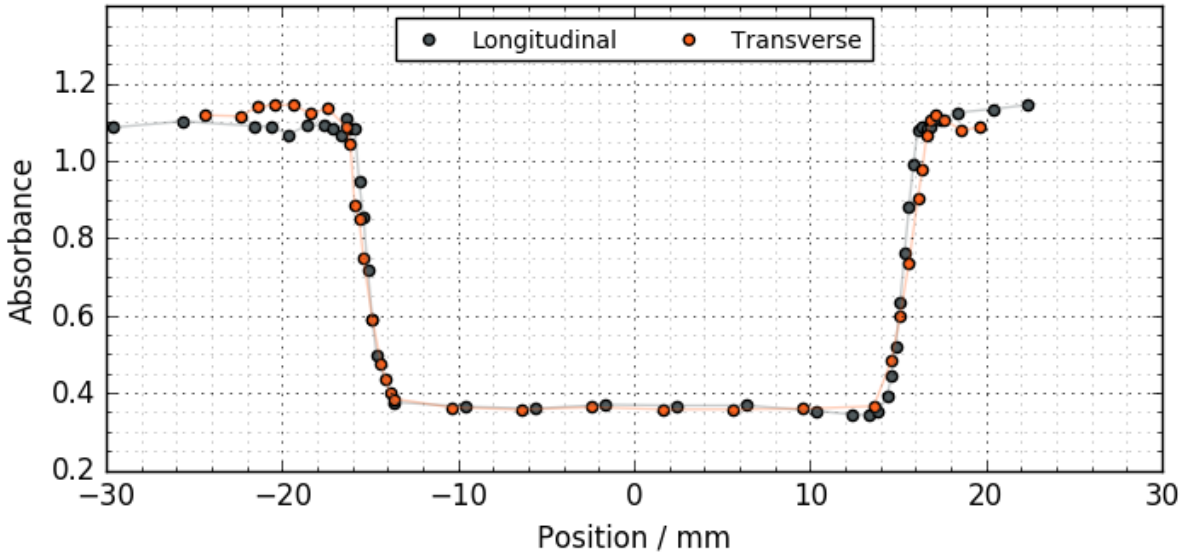

Figure 14: Estimating the size of the field-of-view. Absorbance spectra were taken at different positions moving left-right (transversally) across a 30mm paper strip, and then moving up-down (longitudinally). The absorbance at 2080cm^{-1} is plotted. The profiles were aligned on the midpoint of the trough. The size of the beam can be estimated from the scale of the transition – in both longitudinal and transverse directions, the half-width of this step change is approximately 1mm.

5 Ageing on bituminous samples

5.1 Laboratory Ageing (Rolling Thin Film Oven Test)

5.1.1 IR Spectra

The Extended Rolling Thin Film Oven (ERTFO) Test is an unorthodox method for advancing the aging of bitumen binder. This experiment was carried out at TRL Laboratory at Crowthorne House. A sample of 30/45 Pen grade Bitumen from Esso refinery was heated for ~5 hours in an oven to make it viscous and pourable. This was then transferred into pre-heated and weighed glass vessels. These vessels were placed into the RTFO and when the temperature of the oven reached 163˚C the carriage was started. This was then allowed to run for ~75 mins and then 2 vessels were removed and the carriage restarted for another run. One of these time point samples was allowed to cool to room temperature and weighed; the other was emptied into a small metal container for FTIR analysis. The results of this experiment are shown below:

Table 1: RTFO Test summary

Time in RTFOT (min)	Weight of glass, rod and binder before RTFO test (g)	Time in oven (mins)	Weight of glass, rod and binder after RTFO test (g)	Weight change (g)
75	262.0	75	261.8	-0.2
150	264.0	150	263.8	-0.2
225	262.3	225	262.0	-0.3

Table 1 shows that there was an overall weight loss of 0.3g. This is due to loss of volatile components from the bitumen. This is common during thermal aging of bitumen and contributes to the age hardening of the bitumen. The samples that were taken for analysis via Infra-Red spectroscopy were analysed on a Thermo Scientific Nicolet iS5 with an ATR attachment and the resultant spectra are shown below.

The spectra for the ERTFO test aged bitumen are very similar for all time point samples. However looking closely between the regions 1735-1659cm^{-1} (C=O) and 1064-974cm^{-1} (S=O) there are small peaks emerging close to the baseline. This can be seen in Figure 15 below.

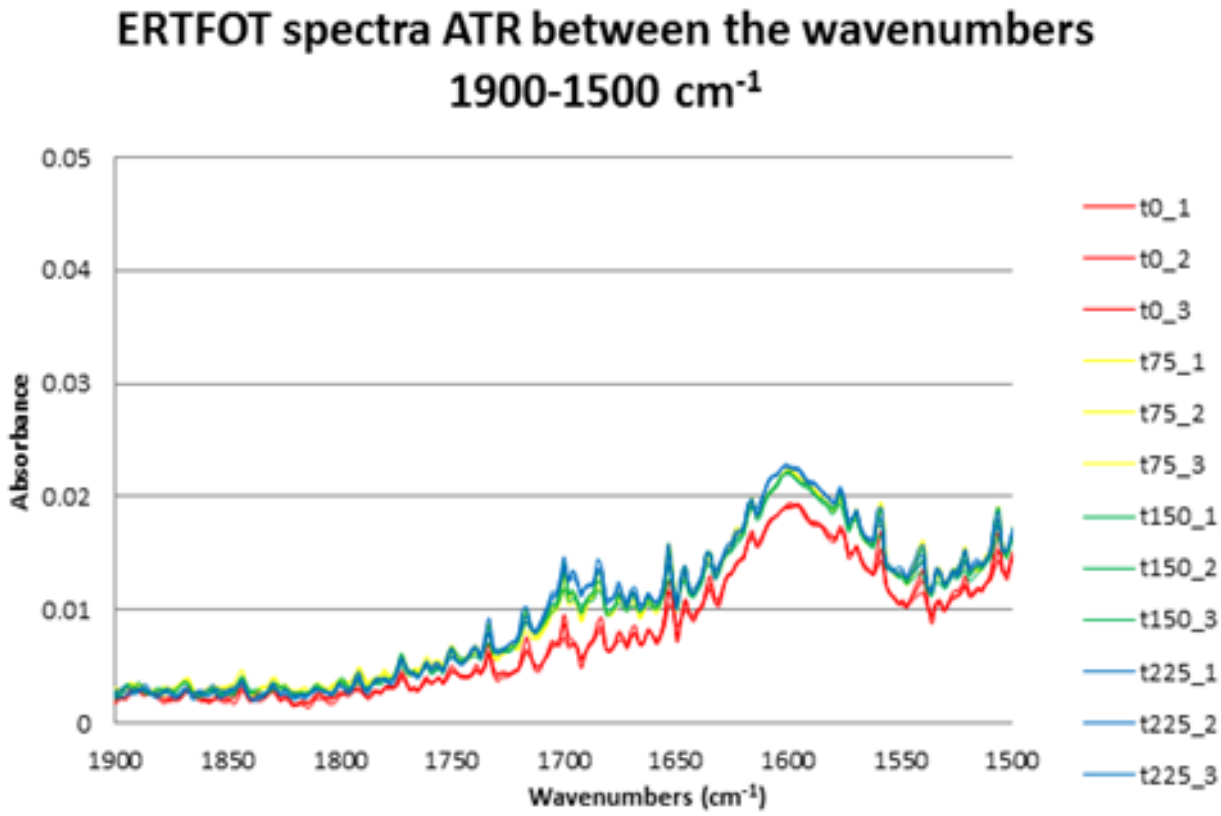

Figure 15: ATR- IR spectra of bitumen at four stages of the extended rolling thin film oven test

The Beer-Lambert law states that absorbance is directly proportional to concentration. Therefore it is possible to quantify the changes in levels of oxidation products forming in the bitumen as the sample is aged by integrating the area underneath an absorbance band. Figure 16 outlines the carbonyl and sulphoxide absorbance band areas from the ATR spectra of the ERTFO test aged bitumen.

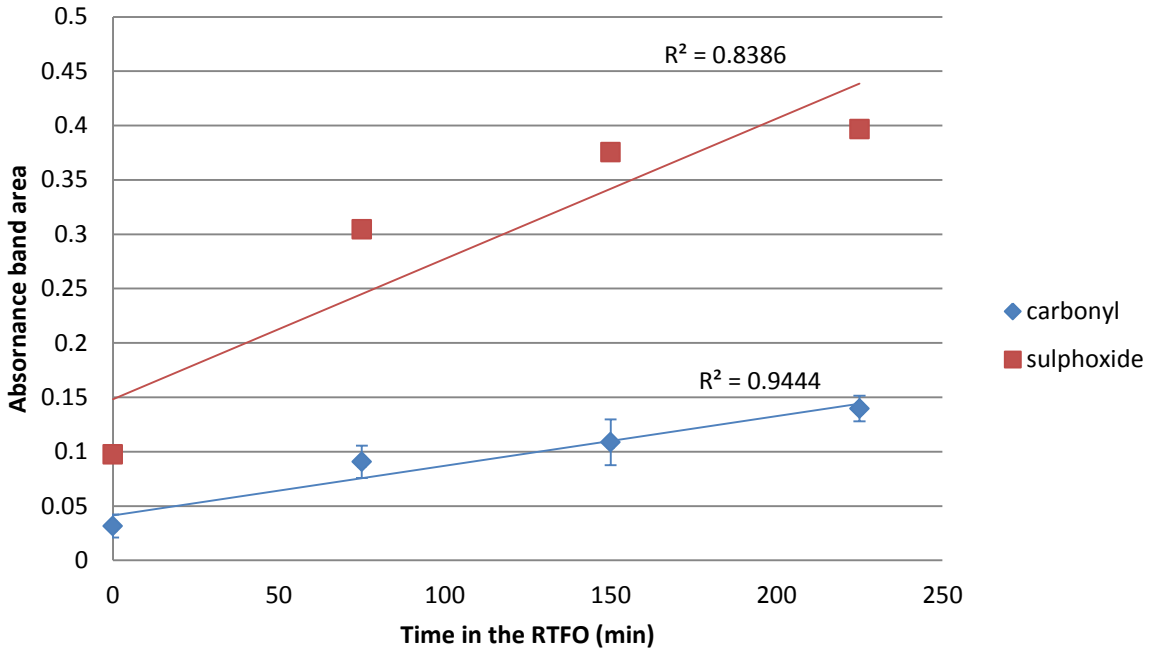

Figure 16: Carbonyl (1753-1659cm^{-1}) and Sulphoxide (1064-974cm^{-1}) absorbance band area analysis from the ERTFO test aged bitumen samples

The integrated area values increase as the time in the RTFOT increases. This supports the trend that many analysts have suggested that the carbonyl peak at approx. 1700cm^{-1} and the sulphoxide peak at approx. 1030cm^{-1} increase as the bitumen becomes oxidised.

5.1.2 Mechanical testing

The penetration and softening points have been measured for the raw bitumen that has been aged in the ERTFO test. The results are shown below in Figure 17.

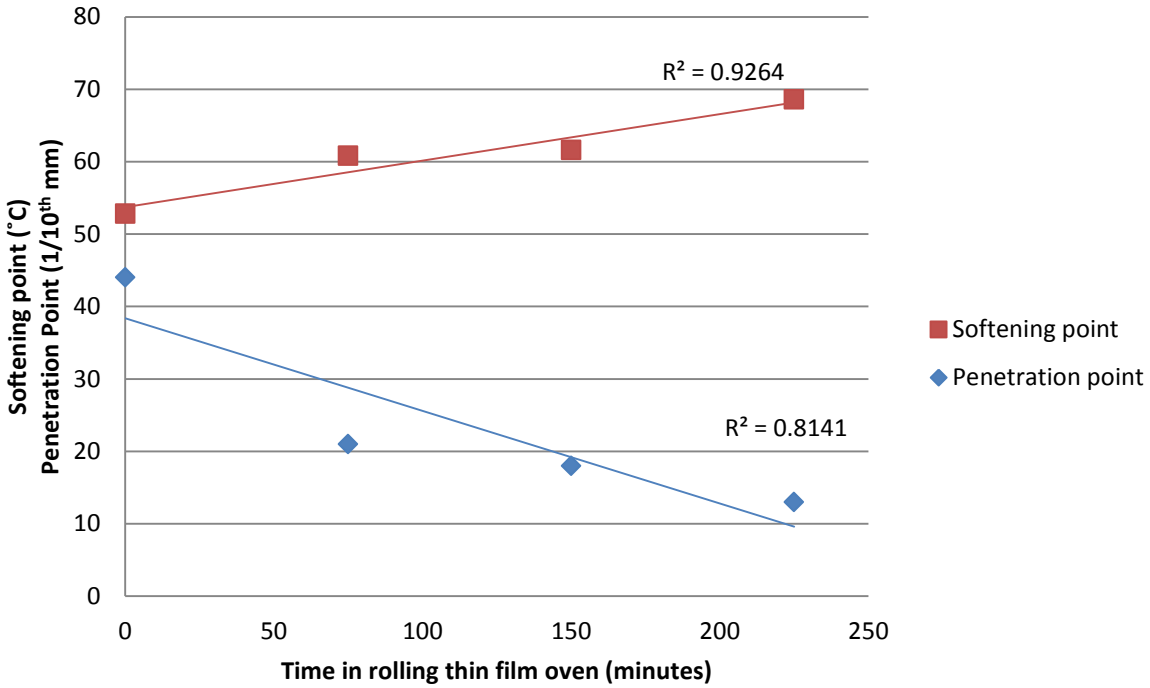

Figure 17: Penetration and Softening point test results of the bitumen aged in the ERTFO test

The data in Figure 17 shows a decrease in penetration point and an increase in softening point. These results suggest that the bitumen is becoming stiffer at lower temperatures.

5.2 Ultra Violet Light Enhanced Ageing of bitumen

5.2.1 IR Spectra

The DRIFT spectra presented in Figure 18 were collected at weekly intervals from the surface of raw bitumen samples that had been aged in the UV chamber. The spectra show many different absorbance bands that correspond to chemical bonds vibrating in the bitumen.

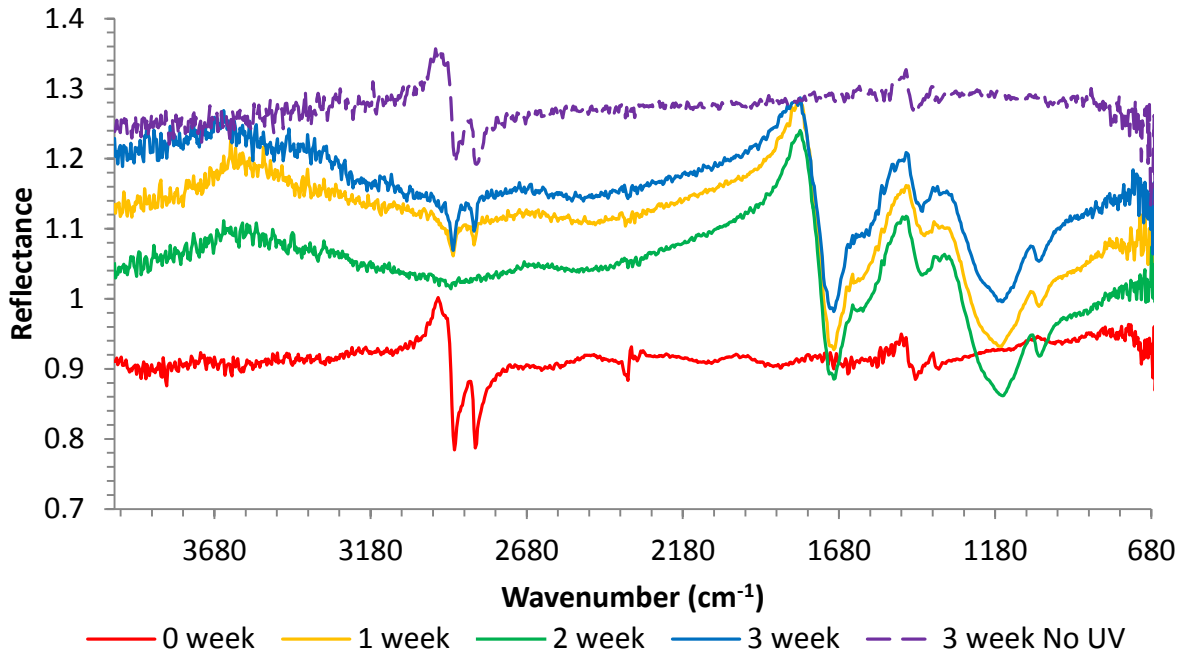

Figure 18: DRIFT spectra from the surface of the raw bitumen samples aged in the UV chamber for 3 weeks

An outline of the absorbance bands and the corresponding bond assignment can be found in Table 2.

Table 2: Outline of the absorbance bands and their bond assignments from the DRIFT spectra shown in Figure 18.

Absorbance Band (cm^{-1})	Bond assignment	
2900, 2840	C-H stretch	Bitumen Hydrocarbon
1735 (centre of 1st derivative peak)	C=O stretch	Oxidation Product
1470, 1380	C-H_2 bending	Bitumen Hydrocarbon
1192	C-O stretch	Oxidation Product
1047	S=O stretch	Oxidation Product

The only absorbance bands present in the unaged bitumen are the C-H stretching and bending modes, found at 2900, 2840 and 1470, 1380cm^{-1}. After one week of ageing in the UV chamber a large first derivative absorbance band appears in the spectrum between the wavenumbers 1980-1650cm^{-1}. This peak has a minimum absorbance at a high wavenumber and a maximum absorbance at a lower wavenumber, 1780 and 1690cm-^{1} respectively. The centre of this first derivative absorbance band is 1735cm^{-1} and this corresponds to a carbonyl bond absorbance. There are also large absorbance bands appearing in the spectra from the aged bitumen between the wavenumbers 1350-970cm^{-1}. This area corresponds to the carboxylic and sulphoxide bonds absorbing at 1192 and 1047cm^{-1} respectively.

It is interesting to note that the spectrum from the surface of the bitumen that had been exposed to 3 weeks' thermal ageing in the UV chamber without the UV light exposure, does

not display the large first derivative feature. This suggests that the formation of the oxidation products requires, or is considerably accelerated by, UV light.

A notable reduction in the intensity of C-H stretch absorbance bands is apparent on exposure to UV, compared with the unaged and thermally aged samples. This is also associated with a change in appearance from first derivative peaks to conventional absorbance peaks, suggesting a reduction in the specular component of the reflection at this wavenumber. This may be associated with a change in the surface reflectance characteristic.

5.2.2 Mechanical testing

5.2.2.1 Penetration and softening tests

Upon ageing in the UV chamber the bitumen produced a visibly non-reflective, brittle 'skin' on the surface of the sample (Figure 19) as a result of leeching of oils to the surface of the sample. The mechanical stiffness of this skin was measured using the penetration point test, the results of which can be found in Figure 20.

Figure 19: Photograph of unaged (left) and 3 week UV aged bitumen (right) samples

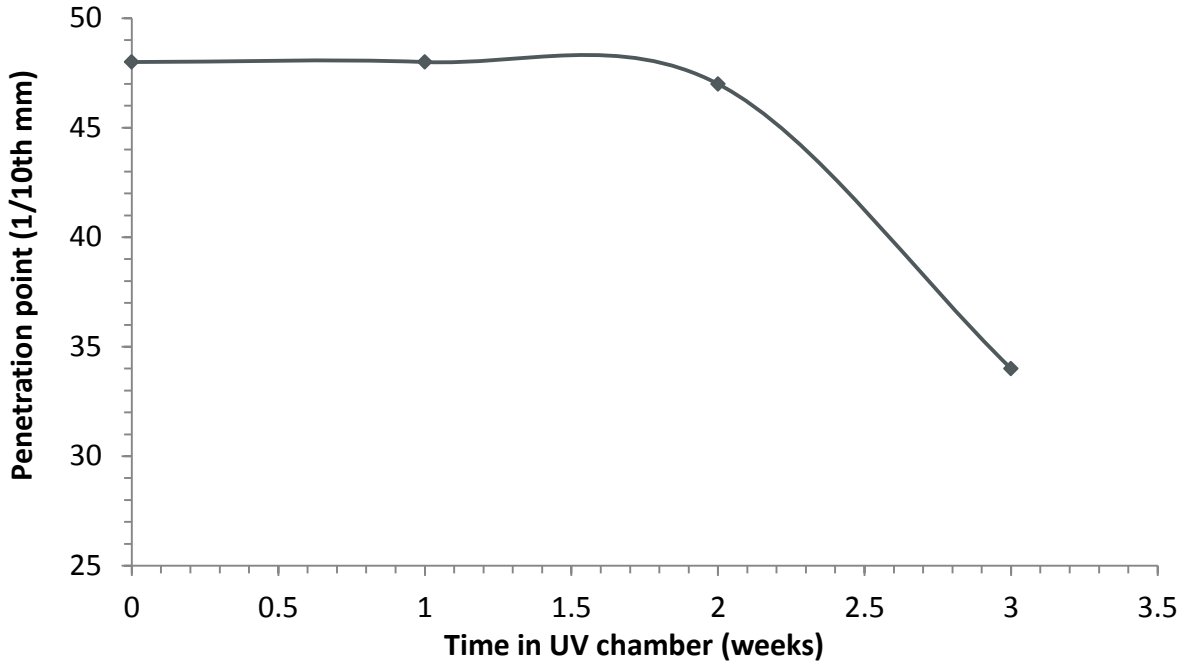

Figure 20: Penetration point from the surface of the raw bitumen after being aged in the UV chamber for 3 weeks

There is a clear drop in penetration point after 2 weeks ageing in the UV chamber. This suggests that there is an increase in stiffness of the bitumen surface after this time. This correlates with the formation of the surface skin and with the oxidation product formation seen in the DRIFT spectra.

The UV enhanced ageing effects mainly the surface of the sample. therefore when carrying out tests such as the softening point and Vialit pendulum test, any mechanical changes that have occurred on the surface are overwhelmed by the bulk properties of the sample. Therefore this data has not been included in this report as there were no significant changes measured with these tests.

5.3 Natural Ageing of bitumen

5.3.1 IR spectra

A similar spectroscopic change can be seen in the DRIFT spectra from the surface of the naturally aged bitumen shown below in Figure 21.

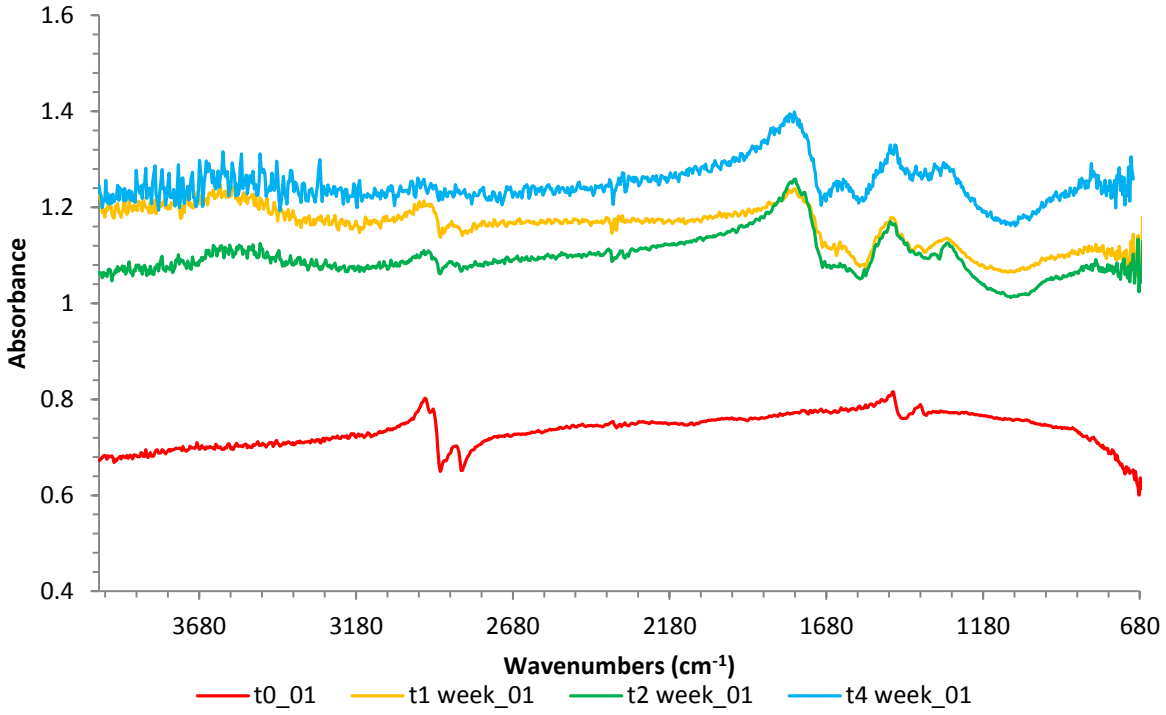

Figure 21: DRIFT spectra from the surface of raw bitumen samples that have been aged naturally on the roof of Crowthorne House, UK

In the unaged raw bitumen spectrum (t0_01) the C-H bending and stretching bands are the only features observed. However, after 1 week of natural ageing there is a large carbonyl absorbance band arising in the spectra. A broad absorbance band can also be seen at ca. 1118cm^{-1} which corresponds to the carboxylic C-O bond absorbing.

For the bitumen samples, the IR spectra clearly demonstrate the emergence of absorbance bands corresponding to the oxidation products of carbon (C=O and C-O) under natural and artificial aging conditions. Under artificial aging, an oxidation product of sulphur (S=O) is also observed.

6 Aging experiments on Asphalt samples

6.1 Ultra Violet Light Enhanced ageing asphalt

6.1.1 IR Spectra

The DRIFT spectra shown in Figure 22 were collected from the surface of UV aged asphalt slabs. They show a number of additional absorbance bands compared to the raw bitumen which correspond to the carbonate filler and siliceous aggregates used to formulate the asphalt.

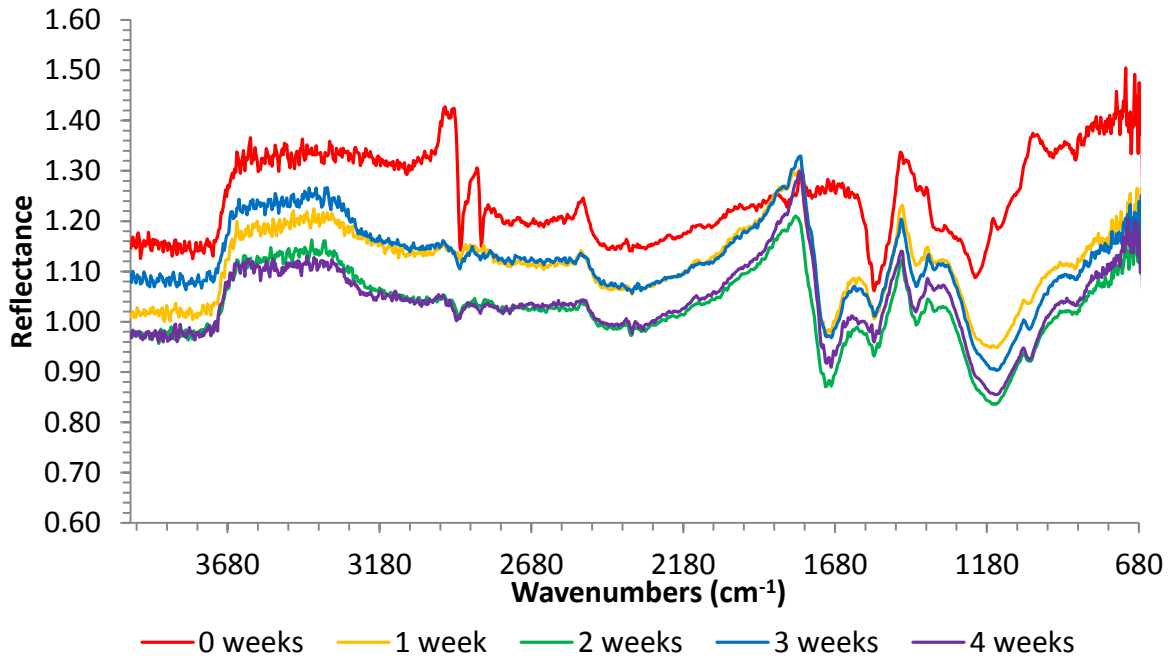

Figure 22: DRIFT spectra from the surface of asphalt that has been aged in the UV chamber for 4 weeks

It is important in this research to be able to differentiate between the carbonyl absorbance from the oxidised bitumen, expected between 1710-1665cm^{-1} wavenumbers, and the CO_3^{2-} combination mode which is expected at approximately 1790cm^{-1} of the calcium carbonate filler. Additional absorbance bands resulting from CO_3^{2-} overtone and asymmetric stretch vibrations are expected at approximately 2510 and 1460cm^{-1}, respectively (Godleman, 2016) (Anderson, 2014).

Table 3 is an outline of the absorbance bands and their bond assignment from the spectra in Figure 23.

Table 3: Outline of the absorbance bands from the DRIFT spectra from the surface of the UV aged asphalt shown in Figure 23

Absorbance Band (cm^{-1})	Bond assignment	
2900, 2840	C-H (stretch)	Hydrocarbon Bitumen
2510	CO_3^{2-} (overtone)	Carbonate filler
1750 (centre of 1st derivative peak)	C=O (stretch)	Oxidation product
1460	CO_3^{2-} (asymmetric stretch)	Carbonate filler
1220	C-O (stretch)	Oxidation Product
1192	Si-O (stretch)	Siliceous Aggregates
1047	S=O (stretch)	Oxidation product
887	CO_3^{2-} (out of plane bend)	Carbonate Filler

It is possible to see the formation of a first derivative absorbance band in the spectra from the UV aged asphalt. This is similar to the result from the UV aged bitumen. It is also possible to assign the absorbance bands from the carbonate and sillaceous filler and aggregates. The absorbance band area between wavenumbers 1826cm^{-1} and 1763cm^{-1}, corresponding to the high wavenumber side of the carbonyl peak, have been integrated and can be found in Figure 23.

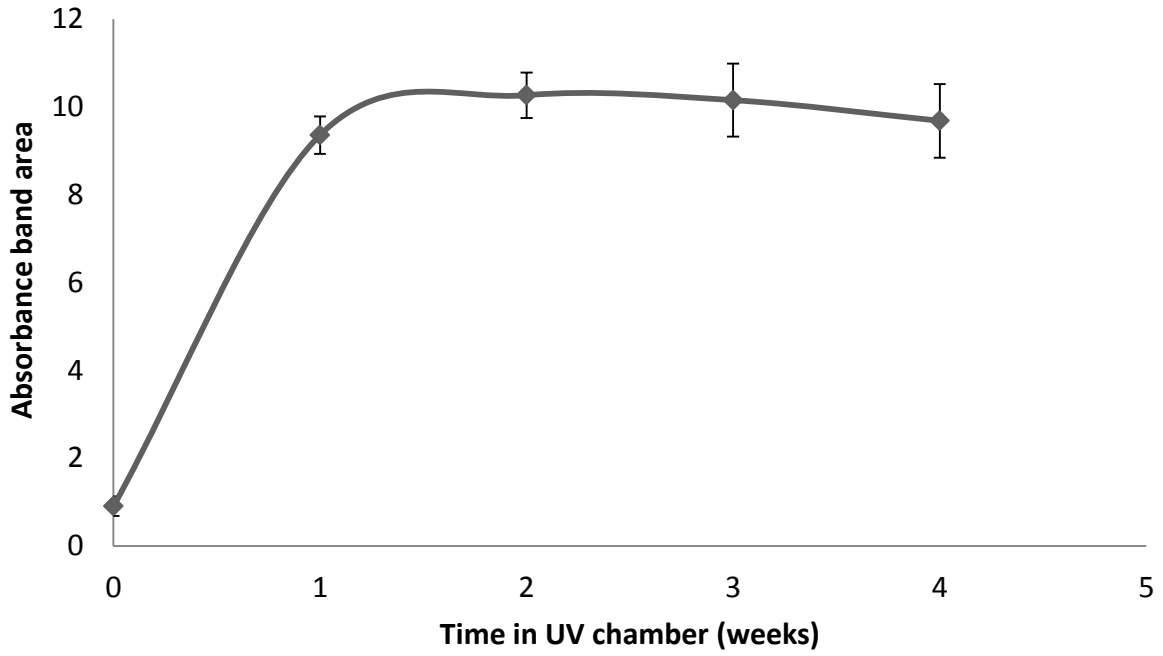

Figure 23: Integrated absorbance band (1826-1763 cm^{-1}) areas measured from the DRIFT spectra from the surface of the asphalt slabs that had been aged in the UV chamber for 4 weeks

It is possible to see a large increase in the area of the carbonyl absorbance band between 0 and 1 week in the UV chamber. This then plateaus and there is little change. This supports what is seen in the DRIFT spectra.

6.1.2 Asphalt shear test results

Figure 24 presents the initial results from the asphalt shear testing of aged (thermal and UV) and unaged (thermal only) samples cut from four asphalt slabs containing the same mixture. The plots represent before and after peak stress development during each test, which are load controlled, against normalised strain (used to remove the effects of seating loads). As the load increases, the linear section at the beginning describes the elastic behaviour of the sample. The curve then transitions smoothly into a nonlinear part which is often characterized by cracking or shear failure. The curve descends linearly as the friction angle drops until it reaches a residual friction coefficient. The curves then become horizontal as there is an increase in strain only.

The results from the testing of the aged (thermal + UV) and unaged (thermal only) samples showed mixed behaviour. The yield (peak) stress and strain values and the slope of the linear elastic section of the curves were obtained by examining the graphs and these are presented in Table 4. Slab A shows some unaged samples having higher yield stress than aged samples, as shown by Figure 24 (a). However, this was not consistent for all samples in slab A or with the results from slabs B, C, and D. Ideally, asphalt samples with high yield stress points tend to have a greater resistance to failure. This behaviour was not observed here on a consistent basis. This was most likely because the effects from thermal ageing in some samples were greater than the effects of UV ageing.

Overall, the average yield stress and strain values are very similar for aged and unaged samples as shown in Table 4. However, the average slope of the linear elastic curves is slightly higher for the unaged samples. The elastic properties of the bitumen contribute greatly to the elastic modulus of the sample as a whole. UV ageing may reduce the elastic modulus of bitumen and therefore contribute to lower cohesion and resistance to failure. More testing is planned which will hopefully provide more insight into the effects of UV ageing on asphalt cohesion. This study would also benefit greatly from a statistical analysis which will be undertaken when more test data is available.

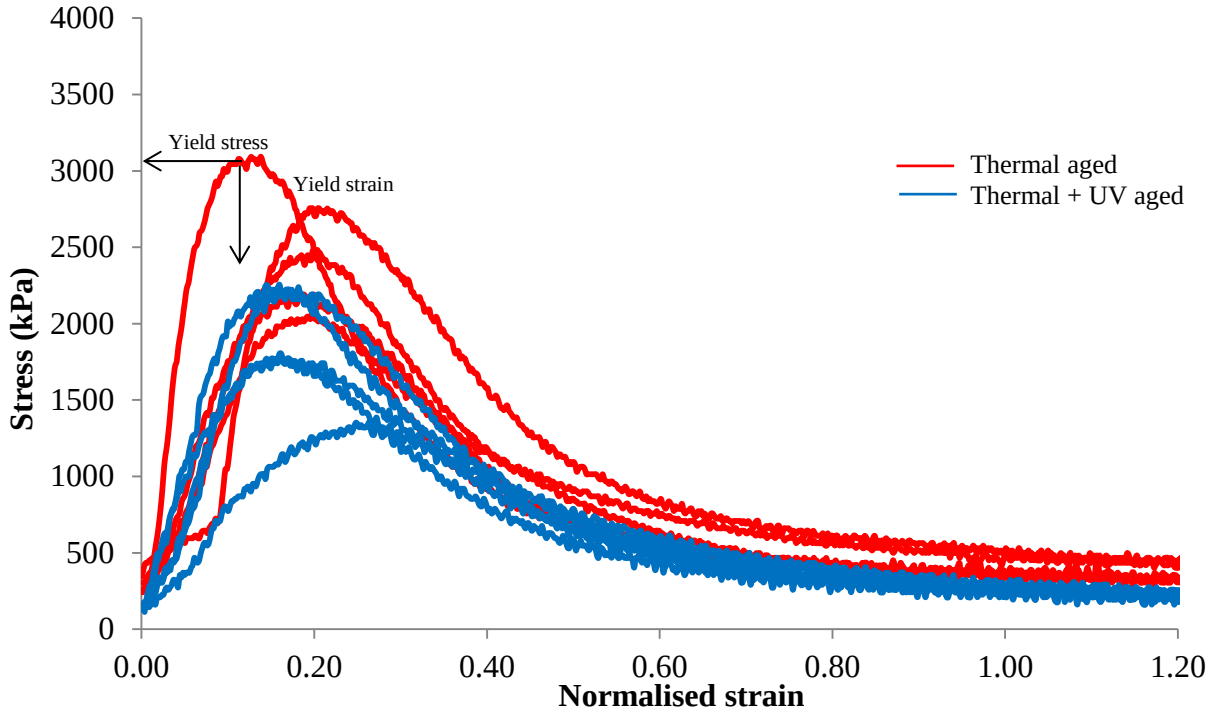

(a) Slab A results – UV & thermal aged vs. thermal aged samples

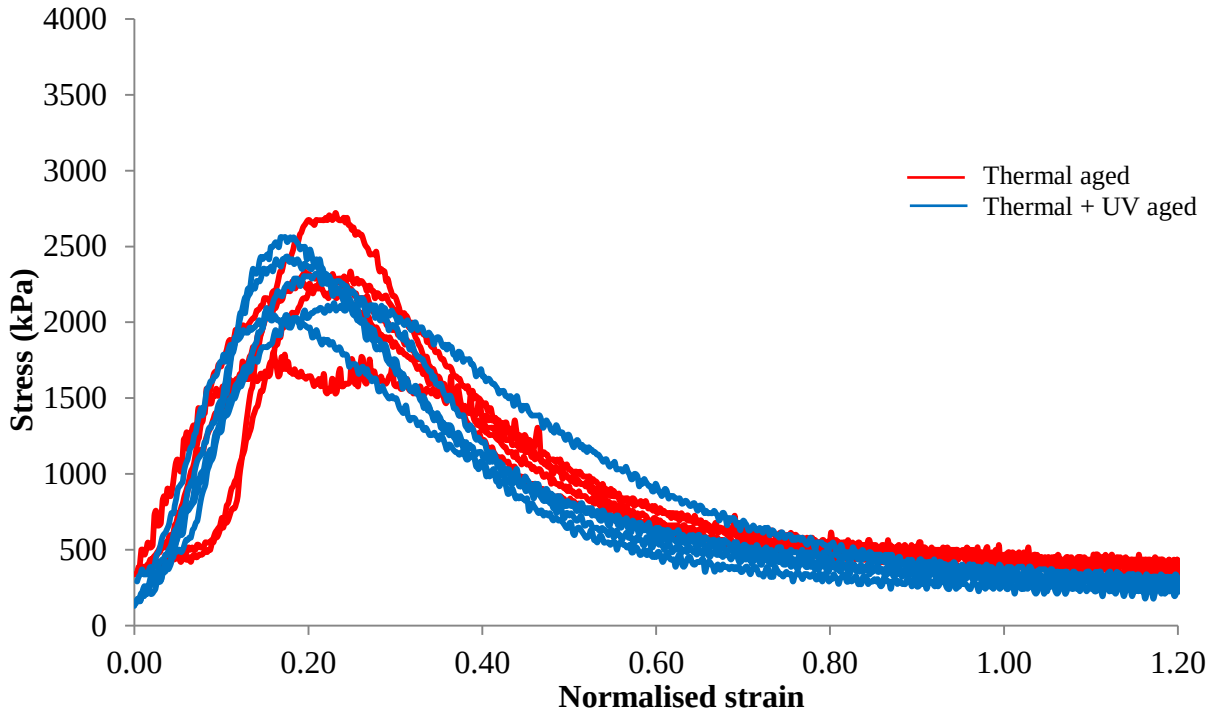

(b) Slab B results – UV & thermal aged vs. thermal aged samples

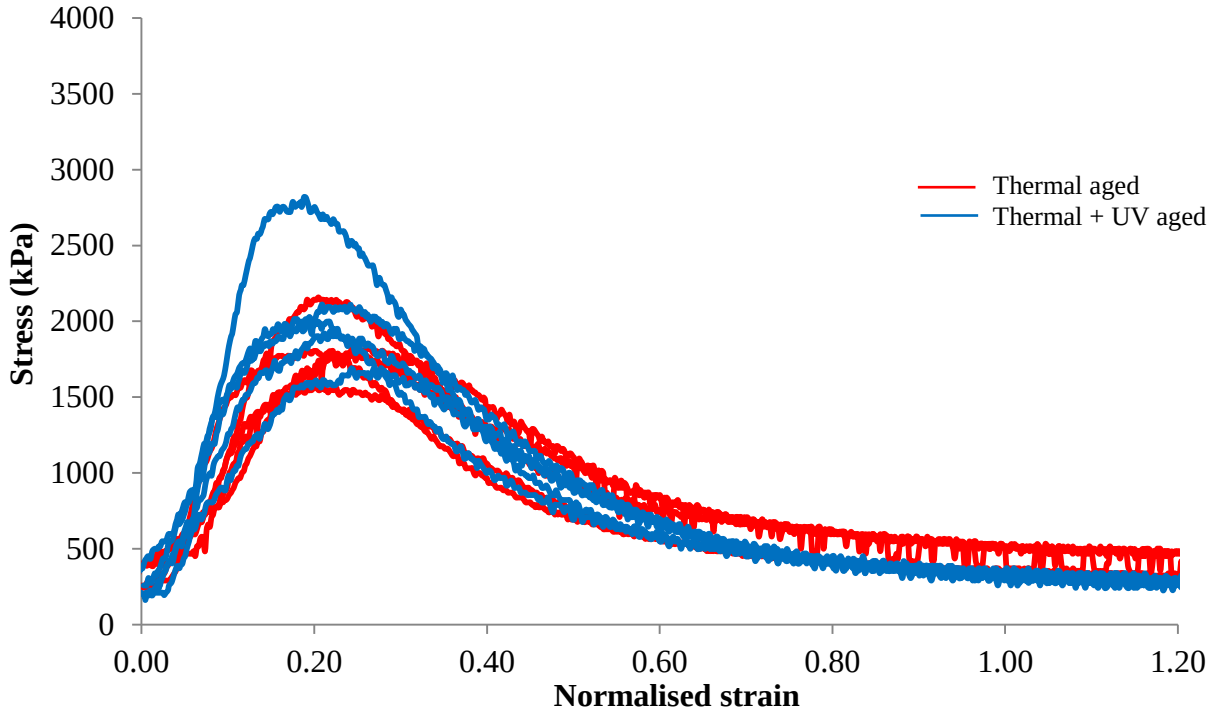

(c) Slab C results – UV & thermal aged vs. thermal aged samples

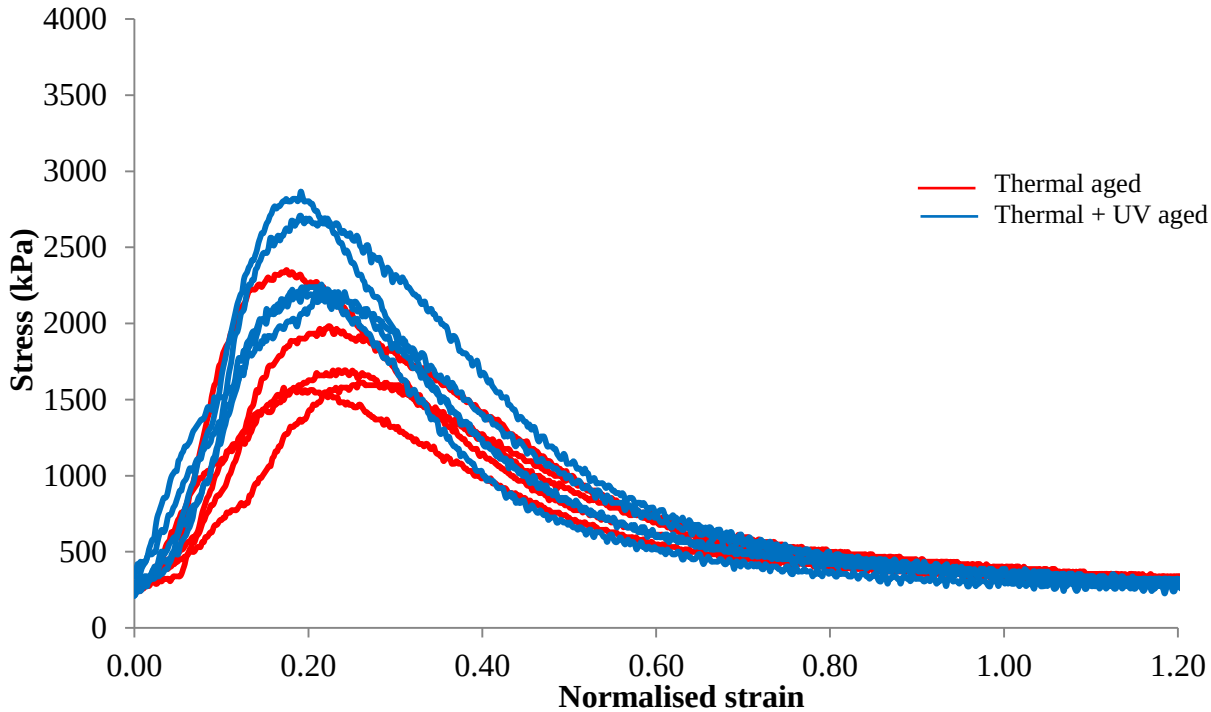

(d) Slab D results – UV & thermal aged vs. thermal aged samples

Figure 24: Stress-strain results from asphalt shear testing

Table 4: Yield stress and strain values and linear elastic slope values from UV aged and thermal aged samples

Thermal aged				Thermal + UV aged			
Sample no.	**Yield stress (kPa)**	**Yield strain (mm/mm)**	**Elastic slope**	**Sample no.**	**Yield stress (kPa)**	**Yield strain (mm/mm)**	**Elastic slope**
A1	2062	0.62	13640	A7	1353	0.70	7142
A2	2754	0.53	32730	A8	2239	0.59	16962
A3	3093	0.34	33455	A9	1772	0.70	16384
A4	2191	0.53	15516	A10	2110	0.62	11774
A5	2480	0.58	15585	A11	2255	0.56	20206
B1	1804	0.41	11515	B6	2319	0.59	14600
B2	2336	0.70	17592	B7	2062	0.50	16964
B3	2722	0.65	38858	B8	2142	0.58	12010
B4	2271	0.65	23497	B9	2561	0.51	24282
B5	2336	0.67	12315	*B10	2432	3.91	2522
C1	1804	0.65	10716	C6	2819	0.62	24101
C2	2158	0.66	16091	C7	2110	0.65	12766
C3	1852	0.65	13058	C8	1691	0.74	7936
C4	1578	0.65	13094	C9	2013	0.58	13672
C5	1804	0.65	19212	C10	1933	0.70	12574
D1	2368	0.72	9908	D6	2867	0.65	21213
D2	1611	0.74	6434	D7	2706	0.62	19121
D3	1981	0.54	13323	D8	2255	0.69	16472
D4	1578	0.65	9456	D9	2239	0.77	14478
D5	2352	0.54	21332	D10	2207	0.65	11173
Mean	2157	0.61	17366	**Mean**	2192	0.63	15465
St.Dev.	406	0.10	8457	**St.Dev.**	360	0.07	5372

Note: St.Dev=Standard deviation, *=test result not included in analysis

6.2 Natural Ageing of asphalt

6.2.1 IR Spectra

Figure 25 shows the DRIFT spectra from the surface of the naturally aged asphalt slabs that were aged for up to 24 months.

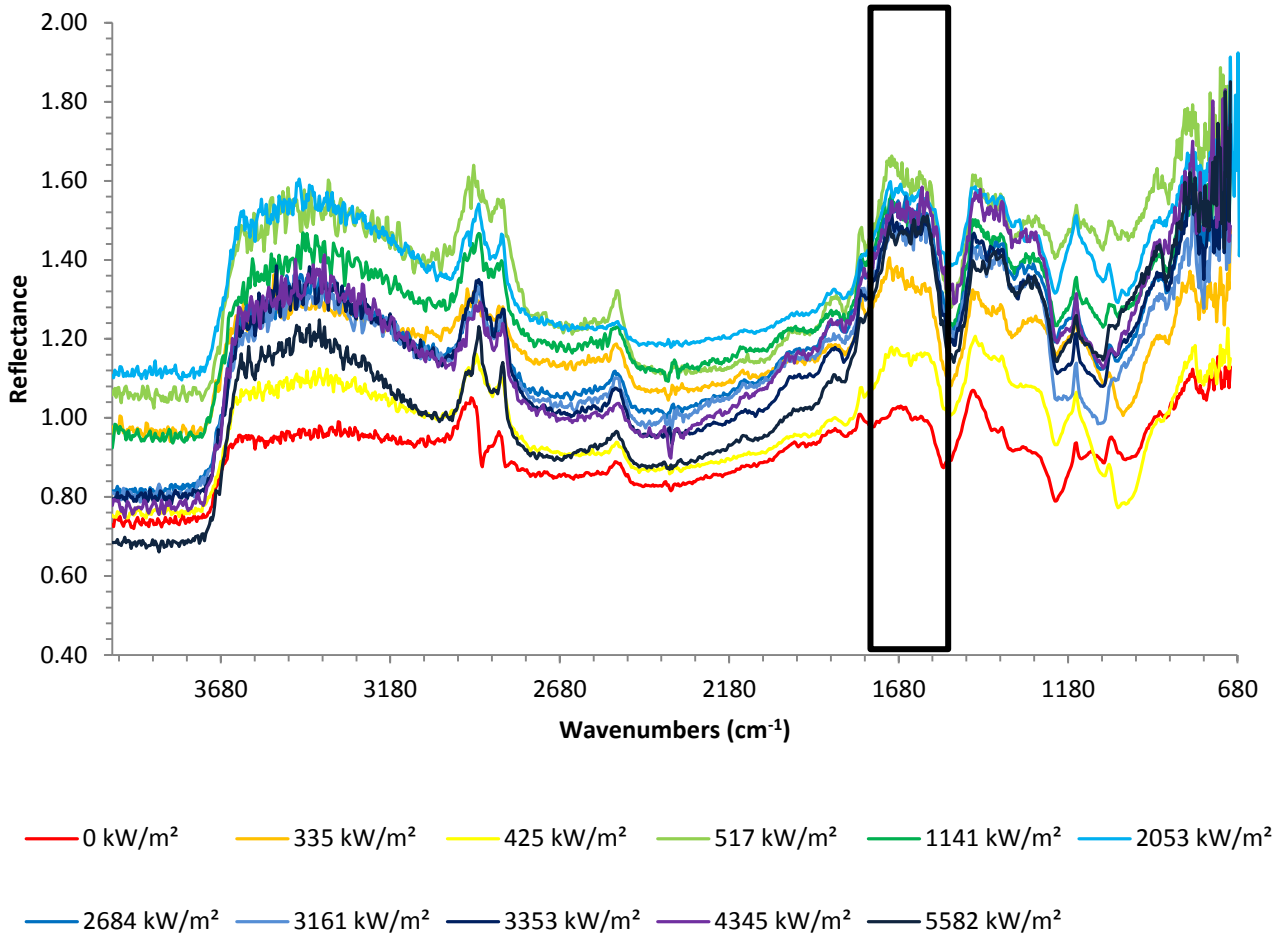

Figure 25: DRIFT spectra from the surface of the asphalt that has been naturally aged on the roof of Crowthorne House, UK

It is possible to see the previously assigned absorbance bands that correspond to the bitumen and aggregates in the spectra shown in Figure 25. The important feature to note is the increase in carbonyl absorbance band area between the wavenumbers 1750 and 1580cm^{-1}. This absorbance band area has been selected for these spectra as the carbonyl absorbance band is presenting as a normal absorbance band as opposed to a first derivative absorbance band, Therefore it is possible to use a wavelength band the centres around the carbonyl absorbance band. This area has been integrated and the results are shown below in Figure 26.

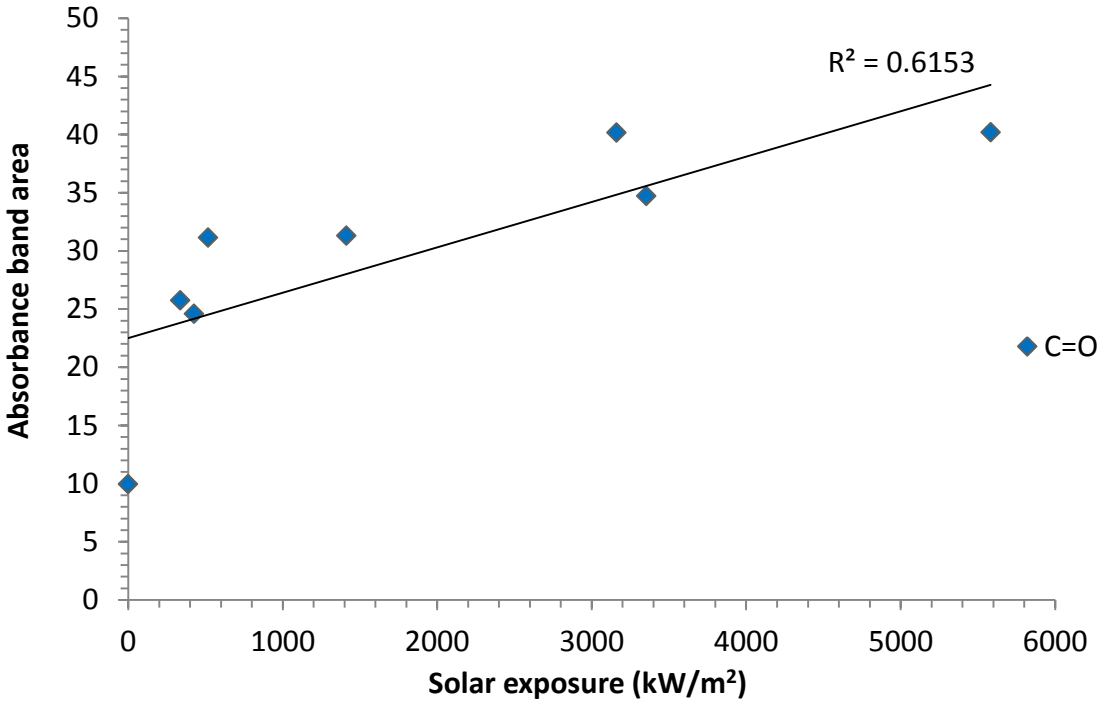

Figure 26: Integrated absorbance band (1750-1580cm^{-1}) areas from the DRIFT spectra from the surface of the asphalt samples that have been aged naturally on the roof of Crowthorne House, vs total solar exposure measured by the weather station at the Transport Research Laboratory

The results in Figure 26 show a gradual increase in the absorbance band area with an increase in solar exposure, which was measured using the weather station. This would suggest that as the samples are exposed to natural UV light the surface is becoming oxidised.

6.2.2 Mechanical testing

6.2.2.1 Penetration and softening tests

The mechanical properties of theses samples have been measured on the bitumen that has been subjected to the binder recovery process. The physical testing results therefore are representative of the bulk of the bitumen as opposed to being isolated to the surface. Figure 27 outlines the penetration and softening points of the naturally aged recovered binder.

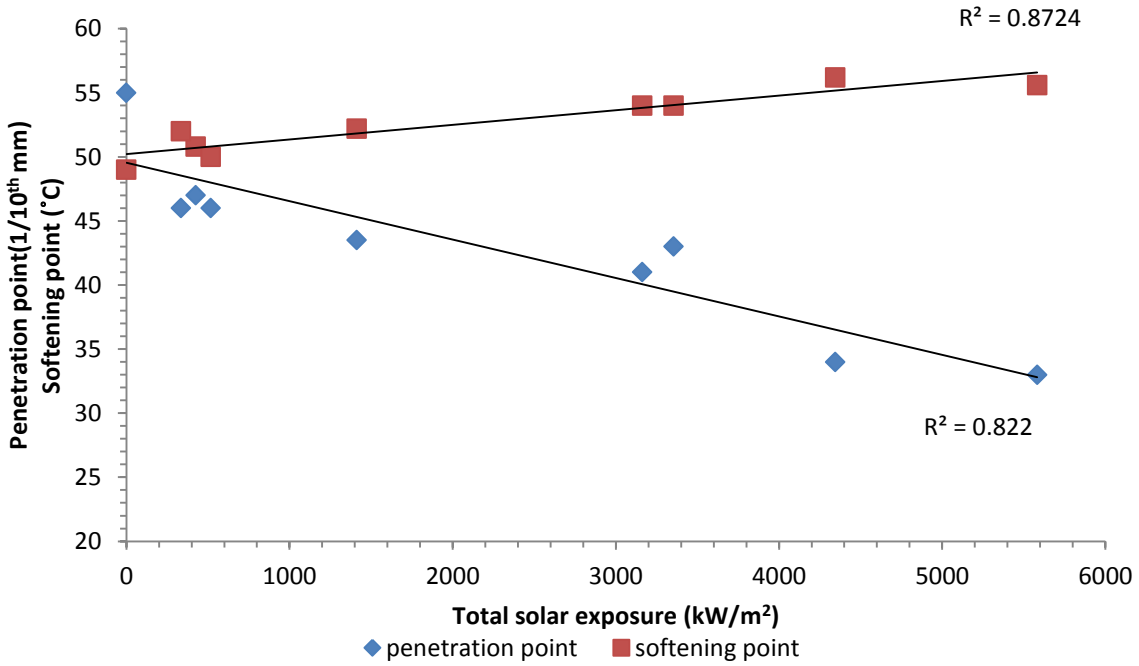

Figure 27: Penetration and softening points of the bitumen recovered from the naturally aged asphalt slabs

It is possible to see a progressive decrease in penetration point and an increase in softening point for the bitumen recovered from the naturally aged asphalt, as the exposure increases. This means that there is an increase in stiffness of the bitumen and a decrease in viscosity at lower temperatures.

6.2.2.2 *Vialit Pendulum test*

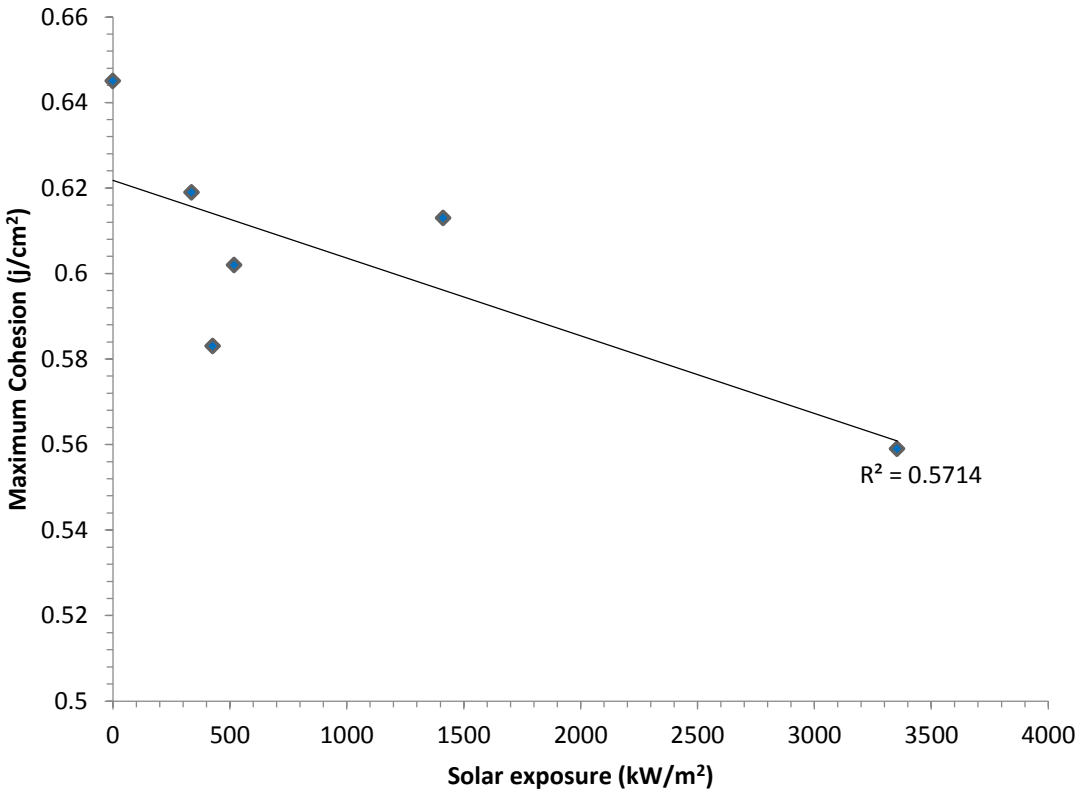

Figure 28: Maximum cohesion of the recovered binder from the naturally aged asphalt slabs, measured with the Vialit Pendulum test

The trend in the maximum cohesion of the recovered bitumen from the naturally aged asphalt is less robust, but indicates a decreasing trend as the asphalt is exposed to an increasing amount of UV light. This reduction in cohesion suggests that as the sample is exposed to more UV light there is a higher chance for physical failures, including fretting.

7 Mobile Spectroscopy

In this section, we will assess the challenges in moving towards an instrument that can be deployed at traffic speed to extract spectral information of road surfaces. The instrument will be required to measure the reflectivity of the road at a finite number of wavelengths in the mid-infrared region. Narrowband interference filters (or similar) will be used to select the individual reflected intensity at the relevant wavelengths, and photodiodes will be used to measure these intensities. Pavement condition will be diagnosed by taking ratios between the different wavelength bands, to normalise the reflected intensity level.

The discussion in this report is split into 3 sections. Section 7.1 examines the general properties of the Exoscan Fourier Transform Infra-Red (FTIR) Spectrometer operating in the diffuse reflectance mode. While the attenuated total reflectance (ATR) method used in earlier experiments requires contact with the sample, the diffuse reflectance method gives the potential to collect spectra at a distance from the sample surface. This is a necessary capability for any practical, traffic-speed solution. Section 7.2 examines the sources of variability in the reflectance spectra. Variability has been observed locally within the sample, and globally across the network. Variability has also been observed due to the instrument. Understanding the effects of variability will help to distinguish changes in the spectrum due to aging distinguished from other variations. Finally, Section 7.3 discusses outstanding issues and recommendations moving towards a prototype instrument.

7.1 Sources of variability

From a proof-of-concept perspective, one of the crucial questions is: can any spectral variation due to aging be distinguished from other sources of variability in the spectrum?

This section will take some steps towards answering this question by discussing some of the sources of variability present in this problem. These can be treated within three loose groupings: variations due to the measuring device; “local” variations within a single pavement sample or test site; and variability at the network-level, due to the different composition of pavements at different sites on the strategic roads network.

Note that it is still unclear what precision will be needed to measure the spectral variations due to aging.

7.1.1 Instrumental variability

In choosing and designing the final measuring device, noise and stability will be two key design requirements. These are, naturally, instrument specific. The Exoscan’s properties were considered in the preceding section, though it is to be remembered that this system is unlikely to be suitable in a traffic speed application.

7.1.2 Local variability within single pavement sample

If useful spectra are to be obtained from a traffic speed survey, it is important to know to what degree a single spectrum is representative of the area around it. This leads to a number of specific questions. For example,

- Could a single spectrum be reported that would reflect the properties of the full lane width over a 10m length?
- Is this methodology reproducible; for example, is it sensitive to changes in driving line?
- As there will be no control over exactly what the measurement is looking at, how much does it matter whether the spectrum is taken on pure binder or on exposed aggregate?
- If, as must be the case in any traffic speed measurement with finite measuring time, each spectrum looks at

7.1.3 Network-level variability between pavement samples

Several points on cores from the same road were scanned and their mean absorbance was plotted on the graph below (Figure 29). The grey lines represent the mean from each core samples and black line represents the mean from all the samples.

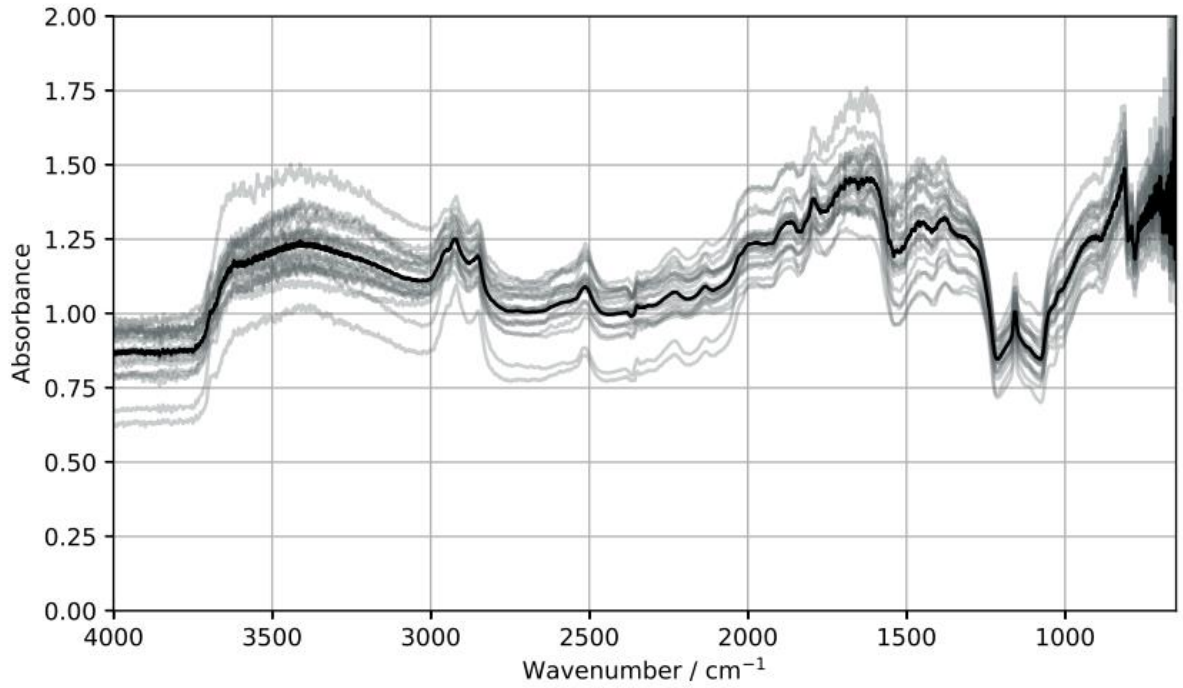

Figure 29: Mean spectrum of samples of the same road

The deviation in the results is as high as 50% for some wavenumbers that shows a substantial variability between cores collected from the same road. This variability can be due different trafficking between lanes, covering of road sections and different road

resurfacing times. As we are measuring the absorbance of a sample at different wavenumbers, samples of the same road have different reflectivity characteristics that will affect the spectrum.

7.2 External contamination

The presence of contaminants on the surface of the road will have an effect on the infra-red spectrum. Common contaminants found on the road will include water, oil, petrol and diesel and any other vehicular liquids. Along with tyre skid marks and mud it is important to be able to differentiate between these contaminants in the infra-red spectra collected from the road.

Water is a very common contaminant due to the frequency of rain in England and the length of time that it takes to evaporate quickly can depend on the temperature of the environment. The spectrum of water is something that is well known and well documented.

Water has a characteristic spectrum with O-H bonds bending and stretching creating absorbance bands at 3300 and 1600cm^{-1} wavenumbers. These peaks are broad due to the effect of the hydrogen bonding between the electronegative oxygen atoms and the hydrogen atoms of neighbouring water molecules.

Liquids that are present in vehicles that could possibly leak onto the road surface include oil, petrol, screen wash, brake fluid, antifreeze and power steering fluid. The volatile components of these different fluids will affect the amount of time that they remain on the road surface. Oil for example will be present on the road for a longer time that a water based screen wash. The ATR spectra of these liquids can be viewed below.

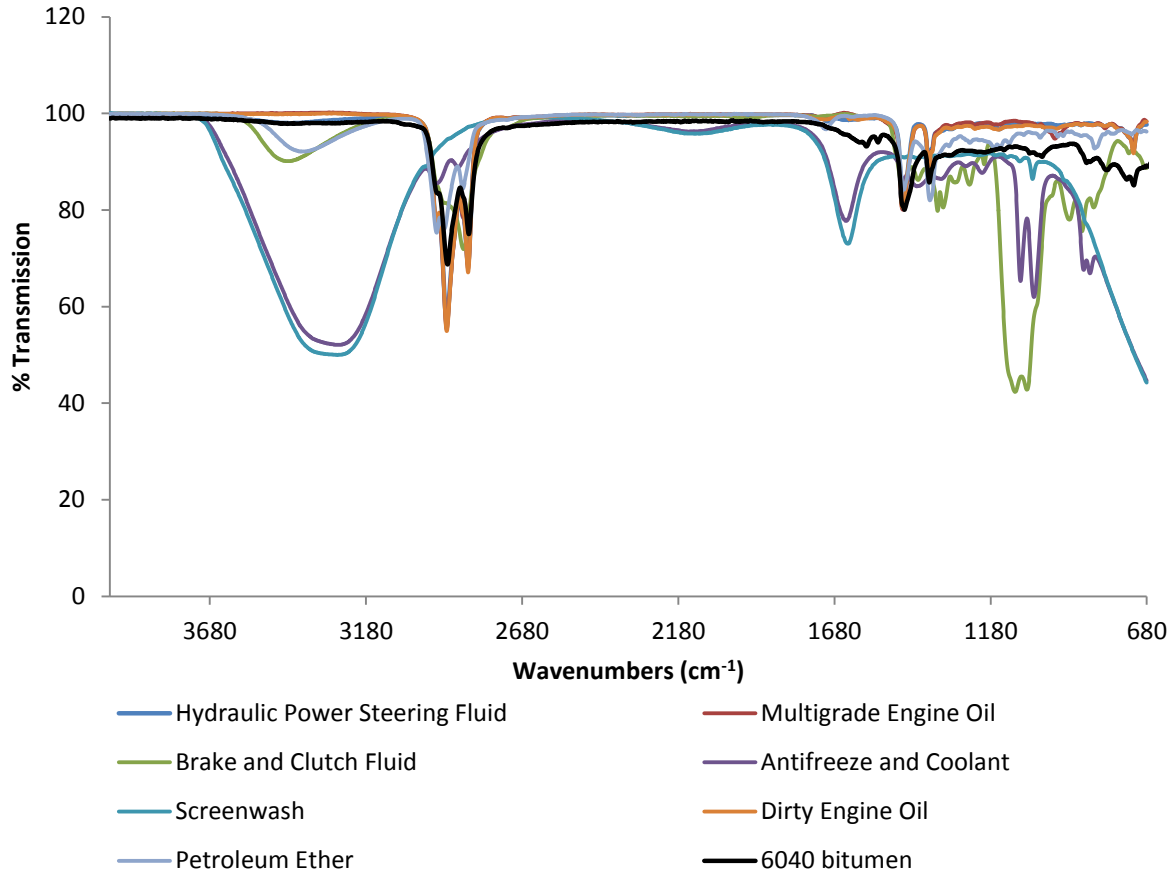

Figure 30: ATR spectra of a variety of different fluids likely to be found on a road surface

Table 5: Outline of the absorbance band locations and the bond assignments from the ATR spectra of the possible road contaminants shown in Figure 30

Absorbance Band (cm^{-1})	**Bond assignment**
3283	O-H stretch (water)
2922, 2854	C-H stretch
1683	H-O-H bend (water)
1457, 1362	CH3 bend
1108, 1061	Si-O stretch
1085,1042	C-O stretch (glycol ether)

Many of the contaminants shown here have peaks that differ from the characteristic peaks in the bitumen. Oil however, shares a similar spectrum as the bitumen due to the oil being made from different length hydrocarbons and therefore having C-H bend and stretch peaks present. When attempting to monitor the oxidation of the bitumen the area of interest would be between 1900 and 1600cm^{-1} which is in an area that is unobstructed by many of the possible road surface contaminants, excluding water. The O-H bending mode of water present in the screen wash and antifreeze shows a large peak at 1683cm^{-1} which may cause interference between the carbonyl absorbance bands if there is water present on the road surface at the time of analysis.

7.3 Construction of a mobile measurement system

In order to move towards a more mobile piece of equipment a trolley had been designed that supports the ExoScan in the correct position and distance above the road surface. This can be moved into position and a spectra can be taken, controlled by a Bluetooth connected PDA. The trolley can then be moved into a new position along the road surface and another spectrum can be collected. This isn't at traffic speed, however it allows an analyst to take spectra along a road surface with ease (Figure 31).

Figure 31: Researcher using the mobile trolley to capture spectra

This trolley has been used to measure a 16m length of car park from the front of the TRL headquarters in Crowthorne House, UK. Below are the spectra collected at 1 meter intervals.

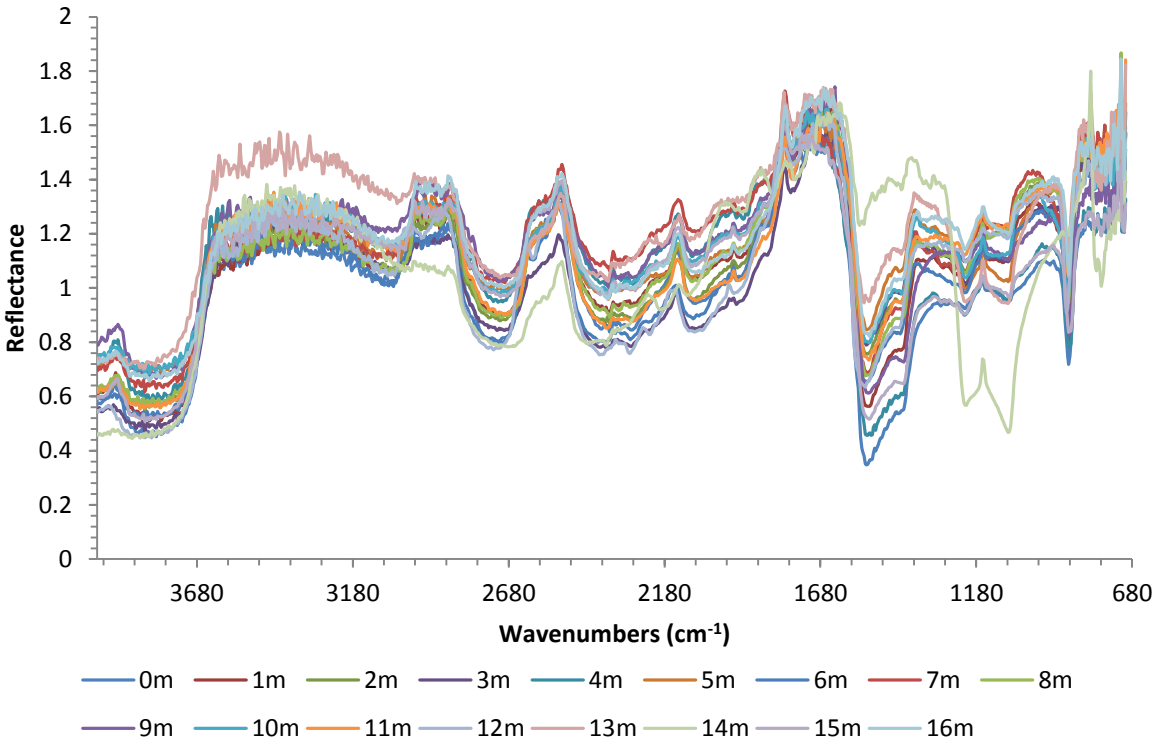

Figure 32: Diffuse reflectance spectra taken from the car park of Crowthorne House, UK, each meter along a 16m stretch

The spectra show similar absorbance bands arising at each meter. There are some variations between the wavenumbers 1300-1000cm^{-1} which corresponds to different levels of exposure of siliceous aggregates. The large absorbance feature between these wavenumbers corresponds to the O-Si-O bond bending, present in siliceous aggregates such as quartz and sand. Changes in areas that are covered predominantly by bitumen will present less absorbance bands that correspond to aggregates and will have strong bituminous C-H hydrocarbon, bending and stretching absorbance bands.

8 Summary, conclusions and Future work

8.1 Summary

The following conclusions can be made from the results presented;

Aged bitumen and Asphalt mechanical testing:

1. As the bitumen is aged in the UV chamber there is a brittle skin forming on the surface. The mechanical stiffness of this skin has been measured using the penetration point test. The results for this show a decrease in penetration point which is indicative of an increase in stiffness of the bitumen's surface. This suggests that bitumen that has been exposed to UV light is stiffer and brittle and therefore more prone to breaking.
2. The recovered binder from these naturally aged asphalt slabs shows a decrease in mechanical properties as the samples are aged. The penetration point is decreasing in value and the temperature of the softening point is increasing as the solar exposure is increasing. The Vialit pendulum test results for this naturally aged recovered binder shows that there is also a decrease in the maximum cohesion for the bitumen. These results suggest a decrease in mechanical ability of the bitumen.
3. The results from the shear testing of the aged (thermal + UV) and unaged (thermal only) samples showed mixed performances. This was most likely due to the overriding effects of temperature and the location of air voids along the failure paths.
4. The average yield stress and strain values were similar for aged and unaged samples. However, the average slope of the linear elastic curves is slightly higher for the unaged samples. This suggests that UV ageing may reduce the elastic modulus of bitumen and therefore contribute to lower cohesive properties.
5. The asphalt shear test showed promise as a method for determining the cohesive properties of asphalt mixtures. However, more testing is required to confirm if this test is robust enough to determine the effects of ageing, temperature, and air void contents.

Spectroscopy:

6. The oxidation functional group absorbance bands are clearly observed in the raw bitumen that has been aged both artificially and naturally. These absorbance bands correspond to the C=O, C-O and, for the artificially aged samples, sulphoxide S=O bond stretches.
7. These peaks are identifiable in the DRIFT spectra of raw bitumen. There are some variations to the appearance of the carbonyl absorbance band due to a difference in physical characteristics of the surfaces being analysed. This peak presents as a first derivative (1972-1679cm^{-1}) when the sample is shiny, for example raw bitumen and UV aged asphalt. This first derivative is a result of a mixture of specular and diffuse reflectance of the IR radiation.

8. The absorbance bands present in the spectra from the asphalt have been assigned to bitumen, calcium carbonate filler and the aggregates. The carbonyl absorbance band (1730cm^{-1}) can be distinguished from the calcium carbonate CO_3^{2-} overtone absorbance band (1789cm^{-1}) by careful interpretation of the spectra.
9. The carbonyl absorbance band can be monitored as the asphalt samples are aged artificially and naturally. This peak presents as a first derivative in the spectra from the UV aged asphalt. However the spectra from the naturally aged asphalt show the evolution of a 'normal' carbonyl absorbance band arising in the DRIFT spectra. This can be seen after only one week of natural exposure.
10. The presence of water and contaminants on the surface of the road would interfere with the spectra and mask some of the important peaks present in the spectra. The absorbance bands of some of these contaminants are shown below:

Absorbance Band (cm^{-1})	**Bond assignment**
3283	O-H stretch (water)
2922, 2854	C-H stretch
1683	H-O-H bend (water)
1457, 1362	CH3 bend
1108, 1061	Si-O stretch
1085,1042	C-O stretch (glycol ether)

11. The internal variation of the road surface may not be larger than the changes due to chemical oxidation.
12. Key absorbance bands for bitumen are shown below

Absorbance Band (cm^{-1})	**Bond Assignment**	
2930, 2840	C-H (stretch)	Hydrocarbon Bitumen
2510	CO_3^{2-} (overtone)	Carbonate Aggregate/Filler
1800	CO_3^{2-} (combination)	Carbonate Aggregate/Filler
1750-1680	C=O (stretch)	Carbonyl oxidation product
1480	CO_3^{2-} (asymmetric stretch)	Carbonate Aggregate/Filler

1220	C-O (stretch)	Carboxylic oxidation product
1160	Si-O (stretch)	Siliceous Aggregates
1090	S=O	Sulfoxide oxidation product
805	CO_3^{2-} (out of plane bend)	Carbonate Aggregate/Filler

Mobile Spectroscopy:

13. The time it takes to measure a full range spectrum between 4000-600cm^{-1} is a few seconds. At traffic speed this could correlate to a distance of a few meters depending on the speed of the vehicle.
14. The distance between the detector and the road needs to be very small for the spectrometer to detect the returning light. When using the ExoScan this distance is approx. 1cm. However when analysing the road at traffic speed this distance needs to be greater in order to prevent damage to the detector.
15. The distance between measurements needs to be considered in terms of getting a clear indication of where on the road surface needs to be treated or resurfaced. The more measurements needed the faster the data needs to be collected at the traffic speed.

8.2 Future work

The initial 2-year SARTS project has made good progress in some difficult areas, and provided a solid foundation on which further developments can be built. However, the work has found that correctly interpreting reflectance spectra, of the type which could be collected in a non-contact, mobile, system is far more complex than initially envisaged in the feasibility study. This has meant that more effort has been required in the lab to develop a full understanding of the processes and data than was initially planned, and less work has been done on developing a mobile system capable of operating on network sites. A follow-up SARTS project will need to:

- categorically demonstrate a link between changes in measured spectra and material performance, extending from bitumen and binder specimens to asphalt;
- develop solutions for the practical issues relating to collection of near-IR spectra in a real world environment;
- collect more spectra from real world sites;
- understand the scales over which a length of pavement can be characterised, leading to an understanding of the spatial data collection requirements;
- monitor a number of sites of different ages and conditions over as long a period as possible, looking for spectral and condition changes and try to link these.

9 Bibliography

Anderson, E. A. (2014). Analysis of wall plasters and natural sediments from the Neolithic town of Çatalhöyük (Turkey) by a range of analytical techniques. . *Spectrochimica Acta Part A: Molecular and Biomolecular Spectroscopy*, 326-334.

Branthaver, J. P. (1993). Binder characterization and evaluation. *Volume 2: Chemistry (No. SHRP-A-368)*.

British Standards Institution . (1990). *BS 1377-7 Methods of test for soils for civil engineering purposes.* London: BSI.

British Standards Institution . (2007). *EN 15323 Accelerated long-term ageing/conditioning by the rotating cylinder method (RCAT).* London: BSI.

British Standards Institution . (2009). *EN 12697-5 Test methods for hot mix asphalt-Part 5: Determination of maximum density.* London: BSI.

British Standards Institution . (2012). *EN 12697-6 Test methods for hot asphalt Part 6: Determination of bulk density of bituminous specimens.* London: BSI.

British Standards Institution . (2015). *EN 1426 Determination of needle penetration.* London: BSI.

British Standards Institution . (2015). *EN 1426 Determination of needle penetration.* London: BSI.

British Standards Institution . (2015). *EN 1427 Determination of the softening point – Ring and Ball method.* London: BSI.

British Standards Institution . (2016). *EN 13108-1 Material specifications - Part 1 : Asphalt Concrete .* London: BSI.

British Standards Institution. (2003). *EN 12697-8 Test methods for hot asphalt Part 8: Determination of void characteristics of bituminous specimens.* London: BSI.

British Standards Institution. (2007). *EN 12607-1 Determination of the resistance to hardening under influence of heat and air. RTFOT method.* London: BSI.

British Standards Institution. (2007). *EN 12607-3 Determination of the resistance to hardening under influence of heat and air. RFT method.* London: BSI.

British Standards Institution. (2008). *EN 13588 Determination of cohesion of bituminous binders with pendulum test.* London: BSI.

British Standards Institution. (2012). *EN 14769 Accelerated long-term ageing conditioning by a Pressure Ageing Vessel (PAV).* London: BSI.

British Standards Institution. (2014). *EN 12607-2 Determination of the resistance to hardening under influence of heat and air. TFOT method.* London: BSI.

Francken, L. (2004). *Bituminous binders and mixes.* London: CRC press.

Godleman, J. A. (2016). An infrared microspectroscopic study of plasters and pigments from the Neolithic site of Bestansur, Iraq. . *Journal of Archaeological Science: Reports,*, 195-204.

Lu, X. &. (2002). Effect of ageing on bitumen chemistry and rheology. *Construction and Building materials,* , 15-22.

Read, J. &. (2003). *The shell bitumen handbook.* Thomas Telford.

Saoula, S. S. (2013). Analysis of the rheological behavior of aging bitumen and predicting the risk of permanent deformation of asphalt. *Materials Sciences and Applications*, 312.

Spragg, R. (2013). *Reflection Measurements in IR Spectoscopy.* Seer Green: PerkinElmer,Inc.

Widyatmoko, D. (2014). *Optical Spectroscopy of Binder Condition at Traffic Speed .*

Spectroscopic Analysis of Roads at Traffic Speed

Other titles from this subject area

PPR643 Detection of changes in pavement texture condition using high resolution 3-D surface measurements, S McRobbie, J Iaquinta, J Kennedy, A Wright, (2013)

ISAP2010 Developing New Methods for the Automatic Measurement of Raveling at Traffic-Speed, McRobbie, S., Wright, A., Iaquinta, J., Scott, P., Christie, C., & James, D, (2010)

PPR740 Use of high-resolution 3-D surface data to monitor change over time on pavement surfaces, McRobbie, S., Wallbank, C., Nesnas, K. & Wright, A. (2015)

TRL ISSN 2514-9652

Crowthorne House, Nine Mile Ride,
Wokingham, Berkshire, RG40 3GA,
United Kingdom
T: +44 (0) 1344 773131
F: +44 (0) 1344 770356
E: enquiries@trl.co.uk
W: www.trl.co.uk

ISBN 978-1-912433-37-7

PPR 860